Progress in Oceanography 187 (2020) 102400

Contents lists available at ScienceDirect

Progress in Oceanography

journal homepage: www.elsevier.com/locate/pocean

Controls on near-bed oxygen concentration on the Northwest European Continental Shelf under a potential future climate scenario

Sarah L. Wakelin[a,*], Yuri Artioli[b], Jason T. Holt[a], Momme Butenschön[b,c], Jeremy Blackford[b]

[a] National Oceanography Centre, Joseph Proudman Building, 6 Brownlow Street, Liverpool L3 5DA, UK
[b] Plymouth Marine Laboratory, Prospect Place, Plymouth PL1 3DH, UK
[c] Ocean Modelling and Data Assimilation Division, Centro Euro-Mediterraneo sui Cambiamenti Climatici, Bologna, Italy

ARTICLE INFO

Keywords:
Dissolved oxygen
Oxygen depletion
Climatic change
Ecosystem processes
Northeast Atlantic Ocean
European continental shelf

ABSTRACT

Dissolved oxygen concentrations in the ocean are declining on a global scale. However, the impact of climate change on oxygen in shelf seas is not well understood. We investigate potential future changes in oxygen on the northwest European continental shelf under a business as usual greenhouse gas emissions scenario (Representative Concentration Pathway RCP8.5). Regions of the European shelf are thermally stratified from spring to autumn, which can cause oxygen depletion in sub-pycnocline waters. A transient climate-forced model simulation is used to study how the temperature, salinity and concentration of near bed dissolved oxygen change over the 21st century. In warming and freshening water, the oxygen concentration declines in all shelf regions. The climate change signal emerges first in salinity, then in temperature and finally in near bed oxygen. Regions that currently experience oxygen depletion (the eastern North Sea, Celtic Sea and Armorican shelf) become larger in the future scenario and oxygen depletion lasts longer. Solubility changes, caused by changes in temperature and salinity, are the dominant cause of reducing near bed oxygen concentrations in many regions. Until about 2040 the impact of solubility dominates over the effects of the evolving ecosystem. However, in the eastern North Sea by 2100, the effect of ecosystem change is generally larger than that of solubility. In the Armorican Shelf and Celtic Sea the ecosystem changes partially mitigate the oxygen decline caused by solubility changes. Over the 21st century the mean near bed oxygen concentration on the European shelf is projected to decrease by 6.3%, of which 73% is due to solubility changes and the remainder to changes in the ecosystem. For monthly minimum oxygen the decline is 7.7% with the solubility component being 50% of the total.

1. Introduction

Dissolved oxygen in the ocean is an indicator of water quality and low concentrations can be a threat to the health of aquatic life. Due to a combination of warmer temperatures, which reduce gas solubility, and an increase in nutrients discharged at the coast, dissolved oxygen concentrations have been declining globally since at least the middle of the 20th century [Breitburg et al., 2018]. [Schmidtko et al., 2017] estimate a reduction of the global oxygen inventory of more than 2% since 1960. Over the 21st century, the global oxygen content is "very likely" to decline [Bindoff et al., 2019; IPCC, 2019] by 3.2–3.7%, for RCP8.5 (Representative Concentration Pathway 8.5 [van Vuuren et al., 2011]) or by 1.6–2.0% for RCP2.6. From 1870 to 2100, in the upper mesopelagic layer, global oxygen is projected to decline by 2–4% [Cocco et al., 2013].

At the sea surface, oxygen concentration is influenced by the exchange of oxygen across the air-sea interface. Marine dissolved oxygen is produced by photosynthesis in surface waters; as phytoplankton sink out of the photic zone respiration exceeds photosynthesis and there is net phytoplankton consumption of oxygen. The phytoplankton are consumed by zooplankton and bacteria, which use oxygen in respiration. Where the ocean is stratified, vertical mixing is inhibited and water below the pycnocline is isolated from atmospheric exchange. In the isolated part of the water column, biological processes may reduce oxygen concentrations to below healthy levels.

A threshold of 2 mg l^{-1}, representing hypoxia, is widely used in the literature, however, many organisms experience hypoxia impacts at higher oxygen concentrations [Vaquer-Sunyer and Duarte, 2008]. For the North Sea [OSPAR, 2003] identified a threshold of 6 mg l^{-1} below which bottom water is defined as oxygen depleted. Coastal regions with oxygen concentrations below 2 mg l^{-1} occur globally [Breitburg et al., 2018] and, within 30 km of the coast, oxygen is currently declining

* Corresponding author.
E-mail address: slwa@noc.ac.uk (S.L. Wakelin).

https://doi.org/10.1016/j.pocean.2020.102400
Received 21 October 2019; Received in revised form 25 June 2020; Accepted 3 July 2020
Available online 10 July 2020

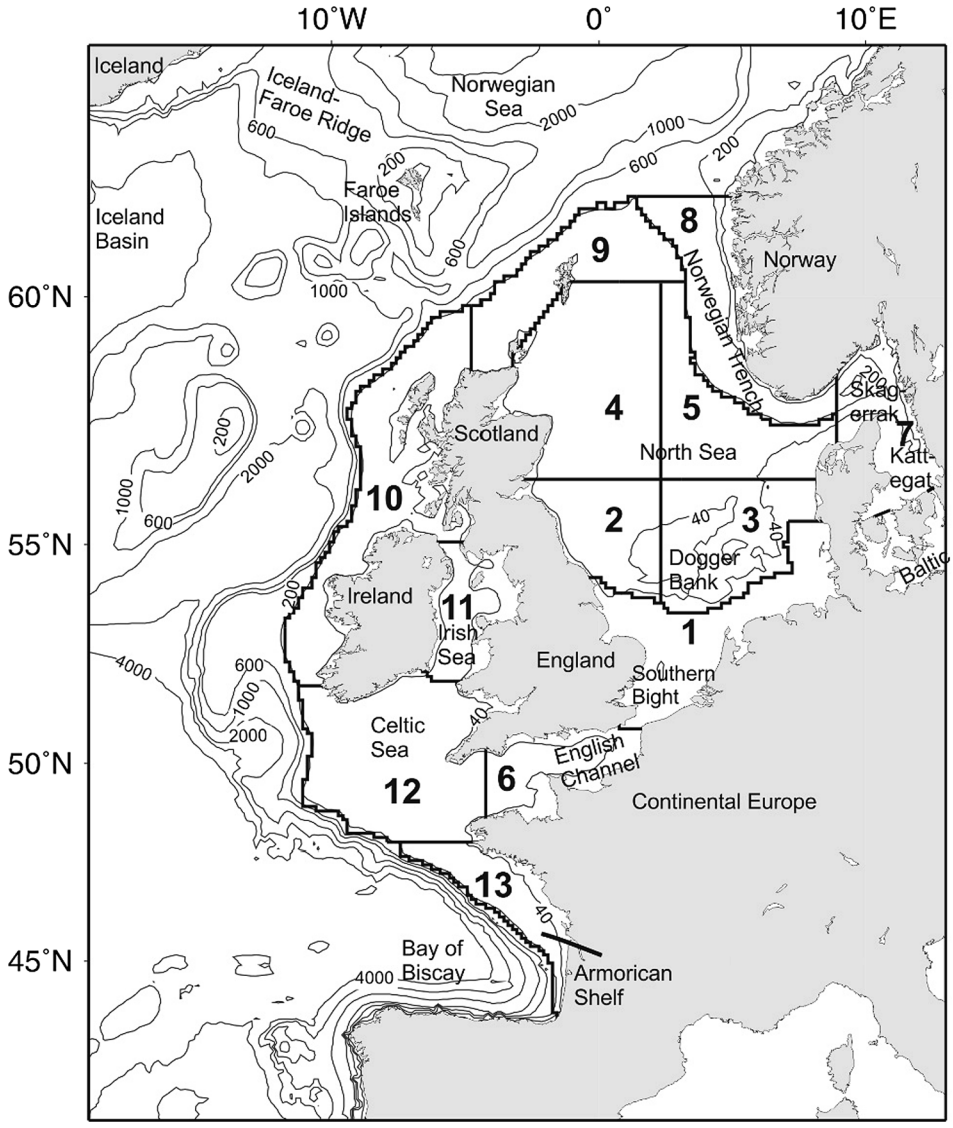

Fig. 1. The AMM7 model domain and bathymetry (in m). The 13 regions used for analysis are also shown.

faster than in the open ocean [Gilbert et al., 2010]. Hypoxia also exists in enclosed and shelf seas (e.g. the Baltic Sea [Carstensen et al., 2014], Black Sea [Capet et al., 2013], North Sea [Topcu and Brockmann, 2015] and Gulf of Mexico [Rabalais et al., 2007]).

The northwest European continental shelf (NWES) is a broad shallow region in the northeast Atlantic (Fig. 1). A northwards flowing slope current runs along much of the edge of the continental shelf, with associated secondary circulation, meanders and eddies contributing to ocean-shelf exchange [Huthnance et al., 2009]. In the Celtic Sea, wind-driven Ekman transport, cross-shelf pressure gradients and Stoke's drift also generate ocean-shelf exchange [Ruiz-Castillo et al., 2019]. Further north, prevailing westerly winds drive on-shelf surface flow and hence downwelling circulation [Huthnance et al., 2009]. On the shelf, the Celtic Sea has a seasonal anti-clockwise circulation [Brown et al., 2003] with a mean flow northwards through the Irish Sea [Brown and Gmitrowicz, 1995; Knight and Howarth, 1999] and eastwards through the English Channel [Prandle et al., 1996]. North Sea circulation is anti-clockwise: Atlantic water enters northeast of Scotland via the Fair Isle Current, the East Shetland Current and along the western side of the Norwegian Trench, joins with inflow from the English Channel and the Baltic Sea, and exits along the eastern side of the Norwegian Trench [OSPAR, 2000; Turrell, 1992]. The transport of Atlantic waters is the major source of inorganic nutrients on the NWES (eg. [Lavín et al., 2006; Ruiz-Castillo et al., 2019; Vermaat et al., 2008]). Other sources are riverine and direct discharge from land (eg. from industry, agriculture and urban wastewater) and atmospheric deposition.

Large areas of the NWES stratify seasonally. The water column is well mixed in the winter, stratifies during spring in response to increasing solar radiation heating surface waters, and remains stratified until autumn when decreasing solar radiation and increased mixing due to storms break down the stratification. During the stratified period oxygen concentrations below the pycnocline can fall to below the oxygen depletion threshold [OSPAR, 2003] in some regions. [Ciavatta et al., 2016] used a decadal model reanalysis to show that parts of the southern North Sea, Celtic Sea, Armorican shelf and English Channel along with coastal zones in Scotland and west of Ireland are vulnerable to oxygen deficiency. [Topcu and Brockmann, 2015] identified thermal stratification, water depth and nitrogen availability as controls on the magnitude of oxygen depletion in the North Sea. [Große et al., 2016] demonstrated that the regions of the North Sea most susceptible to oxygen deficiency are productive regions that are seasonally stratified but with small sub-thermocline volumes, since these store less oxygen than regions with large sub-thermocline volumes at the same oxygen concentrations. Oxygen depletion can potentially be mitigated by reducing terrestrial nutrient sources: [Lenhart et al., 2010] showed that a 50% reduction in riverine nutrient loads increased modelled oxygen

concentrations to above depletion threshold in the southern North Sea.

Climate change has the potential to influence the oxygen cycle in a variety of ways through changes in the hydrodynamic climate (i.e. temperature, salinity, vertical water column structure and circulation) and the impact on biogeochemical cycles. Changes to circulation and stratification affect the nutrient supply and so control phytoplankton production, while changes to water column stratification impact the vertical mixing of oxygen. Gas solubility decreases with increasing temperature, reducing the capacity of water to store oxygen, whereas decreasing salinity increases gas solubility. Biological cycling rates increase with increasing temperature affecting photosynthesis and both autotrophic and heterotrophic respiration. [Helm et al., 2011] estimate that ~15% of current total global ocean oxygen loss is due to solubility change and the remainder is due to increased stratification reducing water mass renewal. [Keeling et al., 2010] estimate that oxygen decline in global climate projections is 2–4 times higher than expected from solubility changes alone. In a model projection to 2100 in the Northern Gulf of Mexico [Laurent et al., 2018] projected that hypoxia would become more severe and prolonged with the main drivers being reduced oxygen solubility (60–74%) and increased stratification (< 40%). The oxygen depletion experienced by regions of the NWES in the present day is a result of combined physical and ecosystem processes. Projected temperature changes will reduce oxygen solubility in the future. However, the response of the ecosystem, in particular the impact of changes in circulation and nutrient supply, could be equally important and reinforce or mitigate the solubility change. Oxygen depletion in regions where oxygen changes are more sensitive to ecosystem processes could potentially be improved by applying regional environmental policies, such as those that limit release of anthropogenic nutrients to the ocean and atmosphere. Here we investigate the relative impacts of solubility and ecosystem changes on oxygen concentrations on the NWES.

We use a coupled hydrodynamic ecosystem model of the northeast Atlantic Ocean to investigate potential changes on the NWES under a climate scenario of comparatively high greenhouse gas emissions (RCP 8.5). We downscale the impacts of potential changes in atmospheric and oceanic climates to the NWES; where future evolution is unknown (e.g. atmospheric nutrient deposition and river flows and nutrient loads) we use present day climatological means. The aims of this study are 1) to estimate the potential decrease in near bed dissolved oxygen by 2100, 2) to investigate how regions of oxygen depletion might evolve and 3) to assess the relative contributions of solubility and ecosystem changes to the oxygen decline. In Section 2 we summarise the main features of the models used and describe the simulations. A method to separate the solubility impacts on near bed oxygen from those due to the ecosystem evolving under physical environment changes is also presented. In Section 3 and Appendix A, we assess the skill of the climate simulation in representing recent past conditions in comparison to a hindcast simulation forced by atmospheric reanalysis. Results are presented in Section 4 and summary and conclusions in Section 5.

2. Methods

2.1. Model descriptions

We use the coupled hydrodynamics-ecosystem model NEMO-ERSEM to model the hydrodynamics and ecosystem of the northeast Atlantic Ocean in the ~7 km-resolution Atlantic Margin Model (AMM7). The domain covers 20°W to 13°E and 40°N to 65°N, including the NWES and the adjacent deep ocean (Fig. 1). The AMM7 model has horizontal resolution 1/15° latitude by 1/9° longitude and uses 32 s-coordinate levels in the vertical [Song and Haidvogel, 1994].

The simulations use version 3.2 of the Nucleus for European Modelling of the Ocean (NEMO) code [Madec, 2008]. A full description of the AMM7 setup is given by [O'Dea et al., 2012]; here we use the model in non-assimilative mode. Tidal forcing is from the equilibrium tide and tidal sea surface elevation and currents from harmonic constants specified at the AMM7 Atlantic boundaries, taken from a north-east Atlantic tidal model [Flather, 1981]. Time-varying open boundary temperature, salinity, surface elevation and barotropic currents are provided by global ocean models (see Section 2.2). Atmosphere forcing is included using COARE3 bulk formulae [Fairall et al., 2003] applied to atmospheric model data (see Section 2.2).

The European Regional Seas Ecosystem Model (ERSEM, [Baretta et al., 1995; Blackford et al., 2004; Butenschön et al., 2016]) is a lower trophic level biogeochemical model which explicitly resolves carbon, nitrogen, oxygen, phosphorous and silicon cycles in a coupled pelagic-benthic system. ERSEM uses four phytoplankton types (flagellates, picoplankton, diatoms and dinoflagellates), three zooplankton types (heterotrophic nanoflagellates and micro and meso zooplankton) and bacteria. The pelagic oxygen cycle comprises the consumption of dissolved oxygen through respiration by phytoplankton, zooplankton and bacteria and the production of dissolved oxygen through photosynthesis. Air–sea fluxes are calculated as the product of the gas transfer velocity [Wanninkhof, 1992; Wanninkhof and McGillis, 1999] and the difference between the oxygen concentration corresponding to saturation at the surface temperature and salinity [Weiss, 1970] and the concentration of oxygen in the surface water.

The coupling of NEMO to ERSEM for AMM7 is described by [Edwards et al., 2012], except that here we use an annual cycle of sediment particulate material and coloured dissolved organic matter from SeaWiFS climatology [Smyth et al., 2006] to calculate non-biotic light absorption [Wakelin et al., 2012] and determine light availability for the ecosystem. The same non-biotic light absorption distribution is used in all model simulations.

2.2. Model experiments

We use three simulations: a hindcast using reanalysis atmosphere and ocean forcing, a climate simulation forced by atmosphere and ocean data from global climate models, and a control run to assess model drift in the climate simulation. The model setups are described in Sections 2.2.1 and 2.2.2, and summarised in Table 1.

Table 1
Summary of model simulations. All simulations use the same present day climatologies of sediment particulate material/coloured dissolved organic matter and rivers.

Simulation	Analysis period	Forcing data			
		Atmosphere	Ocean boundary	Ecosystem boundary	Nitrogen deposition
hindcast	1980–2007	ERA-Interim	ORCA025	climatological	EMEP
RCP8.5	1980–2099	HadGEM2-ES	NEMO-MEDUSA	NEMO-MEDUSA	EMEP (to 2009 then 2009 repeat)
CTL	1980–2099	HadGEM2-ES (1980 repeat)	NEMO-MEDUSA (1980 repeat)	NEMO-MEDUSA (1980 repeat)	EMEP (1980 repeat)

2.2.1. Reanalysis-forced simulation

The hindcast uses surface forcing from the ERA-Interim global atmospheric reanalysis [Dee et al., 2011]. Open boundary conditions for temperature, salinity, currents and surface elevation are taken from a 0.25° global NEMO implementation (ORCA025-N206, [Blaker et al., 2015]). Open-boundary nutrient (nitrate, silicate and phosphate) and dissolved inorganic carbon (DIC) values are derived from climatologies [Garcia et al., 2006; Key et al., 2004], providing an annual cycle of monthly values for each component. Atmospheric nutrient deposition data for dry and wet deposition of oxidised and reduced nitrogen are from the European Monitoring and Evaluation Programme (EMEP) Cooperative Programme for Monitoring and Evaluation of the Long-range Transmission of Air Pollutants in Europe, downloaded from http://www.emep.int/. A climatological annual cycle of freshwater river fluxes at daily frequency is derived from daily discharge data for 250 rivers from 1984 to 2004 (Global River Discharge Data Base [Vörösmarty et al., 2000]) and from data prepared by the Centre for Ecology and Hydrology as used by [Young and Holt, 2007]. The Baltic flows at the south of the Kattegat are treated as additional rivers. An annual cycle of daily nutrient concentrations is derived for each river from data used by Lenhart et al. [2010] covering the period 1984 to 2004, including data processed by van Leeuwen (NIOZ & Utrecht University, pers. comm) for the UK, Northern Ireland, Ireland, France, Norway, Denmark and the Baltic and by [Pätsch and Lenhart, 2004] for Germany and the Netherlands.

The hindcast starts from rest in January 1970 using initial temperature and salinity fields from the ORCA025 simulation and initial ecosystem fields from a previous AMM7 simulation where homogeneous initial values corresponding to the average bulk properties of the shelf are spun up for five years. The simulation runs to 2007, which is the last year of the ORCA025 simulation that supplies boundary data. To give the model time to adjust from initial conditions, we discard the first 10 years in the analysis.

2.2.2. Climate projections

For the climate projection simulations, the model is forced with atmosphere, ocean and ecosystem boundary data consistent with Representative Concentration Pathway (RCP) 8.5 [van Vuuren et al., 2011], where greenhouse gas emissions continue to rise throughout the 21st century. Atmospheric forcing is from a simulation of the UK Met Office's HadGEM2-ES Earth System model used in the Coupled Model Intercomparison Project 5 (CMIP5) [Jones et al., 2011]. HadGEM2-ES is a global coupled atmosphere-ocean general circulation model with atmospheric resolution of 1.875°×1.25°. Ocean boundary data are downscaled by using data from a 1° × 1° global simulation of the coupled hydrodynamic-ecosystem model NEMO-MEDUSA [Yool et al., 2013], which uses atmospheric forcing data from the RCP8.5 HadGEM2-ES simulation above. Atmospheric pCO_2 values under RCP8.5 for 1979 to 2100 [Riahi et al., 2007] were downloaded from the RCP database (http://www.iiasa.ac.at/web-apps/tnt/RcpDb). In the absence of climate projections for river data, the river outflows and nutrient loads are the same as used in the AMM7 hindcast. The atmospheric nitrogen deposition dataset used for the hindcast showed steady decline in values from 1980 to 2009. The climate projection used the same nutrient deposition data as the hindcast upto 2009 and then 2009 values for 2010 onwards.

For the RCP8.5 simulation, the model starts from rest using initial temperature and salinity fields from NEMO-MEDUSA for January 1980. Initial ecosystem fields are the same as used in the hindcast. AMM7 is spun-up for 10 years using repeated forcing for 1980, and then run forwards from 1980 to the end of 2099.

A control simulation is used to assess the magnitude of changes due to the oceanic and atmospheric climate as distinct from changes due to model drift over the long (120 year) simulation. Model drift is potentially due to imbalances in the solution of equations (eg from approximating derivatives by discrete expressions to be solved numerically) and parameterisations (eg deposition and resuspension of organic particulates that are not in balance because there is net transfer between benthic and pelagic pools). Adjustment to initial conditions can also be a source of model drift, which we minimised by spinning up the model for 10 years for the hydrodynamics and 15 years for the ecosystem. Model drift is the change in the model fields in the absence of changes in external forcing and is also partly a response to imbalances in the evolving marine environment. We assess model drift by forcing the model with a single annual cycle of forcing data and looking for trends in model output. The control simulation (CTL) runs for 120 years from the end of the spin-up period (1980) and uses repeated atmospheric (including nutrient deposition and pCO_2) forcing and oceanic boundary data for the year 1980.

2.3. Solubility and ecosystem controls on near bed oxygen

Through their impact on oxygen solubility in water, temperature and salinity are strong controls on dissolved oxygen concentrations. On the NWES, temperature and salinity are affected by atmospheric processes, hydrodynamics (such as ocean circulation and stratification) and river outflows. We use the temperature/salinity dependence of oxygen solubility to estimate the relative importance of solubility controls and ecosystem processes on near-bed oxygen concentrations. The method is based on the idea of apparent oxygen utilization (AOU) defined as the difference between oxygen concentration at saturation and the actual oxygen concentration which has been affected by biological activity.

To approximate the temperature/salinity controls on the oxygen concentration we represent the dissolved oxygen at each model grid point as the product of a fixed annual cycle (representing recent past conditions) and a function that depends on the near-bed temperature and salinity as they evolve in time.

For each month, the oxygen saturation state is calculated from $DO_s = DO/SO(T, S)$, where DO is the oxygen concentration from the model simulation and $SO(T, S)$ is the oxygen solubility [Weiss, 1970] at the near-bed temperature (T) and salinity (S). The reference annual cycle of monthly oxygen saturation ($DO_{s,RP}$) is the oxygen saturation in each calendar month, DO_s, averaged over 1980 to 2009. $DO_{s,RP}$ represents the recent past (RP) oxygen saturation state due to the combined impact of ecosystem processes and the physical climate. The RP period was chosen to be as close to the hindcast period as possible so that average conditions from the RP in the climate simulation could be compared to average hindcast conditions for model validation.

For each month of the period 1980 to 2099, we define the oxygen concentration resulting from a combination of average ecosystem processes in the RP ($DO_{s,RP}$)and evolving solubility (SO) to be

$$DO_p = DO_{s,RP}.\ SO(T, S) \tag{1}$$

where the value of $DO_{s,RP}$ appropriate for the month of year is used and $SO(T, S)$ is calculated from temperature and salinity in each month from 1980 to 2099. DO_p is the expected oxygen evolution from 1980 to 2099, assuming that the saturation state does not change, and represents the solubility component of dissolved oxygen. ΔDO_p is the change in oxygen concentrations from temperature and salinity changes alone, in the absence of any changes to the ecosystem. The difference

$$\Delta DO_e = DO - DO_p \tag{2}$$

is the time evolution of changes in the saturation state for 1980 to 2099. If the water mass composition does not change, $\Delta DO_e$is associated with changes in the ecosystem relative to mean RP conditions. ΔDO_e includes the impact of changes to the ecosystem from changing hydrodynamic conditions, e.g. temperature (affecting metabolic rates and the carbonate system), salinity (affecting the carbonate system) and circulation/mixing (affecting nutrient supply).

The dependence of annual mean oxygen concentration on temperature and salinity, DO_p^{ann}, is calculated from (1). The change in DO_p^{ann} due to temperature/salinity changes since the RP is defined by

$\Delta DO_p^{ann} = DO_p^{ann} - \overline{DO_p^{ann}}$, where $\overline{DO_p^{ann}}$ is the average of DO_p^{ann} during the RP; the annual mean change due to ecosystem changes from the present day ΔDO_e^{ann} is calculated from (2).

The solubility/ecosystem evolution of minimum oxygen is studied by selecting, for each model grid point, the month during the 1980 to 2009 period where the mean oxygen concentration is smallest (e.g. October for much of the shelf, Fig. 12i). The evolution of minimum oxygen due to temperature/salinity changes DO_p^{min} is calculated from (1) using the reference oxygen saturation, temperature and salinity for the chosen year-month. The impact of evolving temperature and salinity is $\Delta DO_p^{min} = DO_p^{min} - \overline{DO_p^{min}}$, where $\overline{DO_p^{min}}$ is the average of DO_p^{min} during the RP; the ecosystem impact ΔDO_e^{min} is calculated from

$$\Delta DO_e^{min} = DO^{min} - DO_p^{min}$$

where, for each year, DO^{min} is the dissolved oxygen in the month of minimum oxygen.

3. Model skill

The version of AMM7 used here has been validated for hindcast simulations [Edwards et al., 2012; O'Dea et al., 2012] and found to demonstrate skill in representing physics (tides, temperature and salinity) and ecosystems (nutrients and chlorophyll-a) for the NWES. For climate scale simulations we validate (Appendix A.1) by comparing to climatologies generated using observations from the World Ocean Database (WOD) [Boyer et al., 2013] and find that the hindcast and RCP8.5 simulations are generally too warm and too fresh. Shelf mean temperature/salinity biases of 0.4 °C/−0.1 (0.8 °C/−0.2) and RMS differences of 1.2 °C/0.8 (1.5 °C/0.8) for the hindcast (RCP8.5) are of the same order as for the earlier hindcast [O'Dea et al., 2012]. Biases and RMS differences are generally greater in RCP8.5 than in the hindcast possibly due to the existence of long period natural variability not captured by the climate simulation and to the atmospheric climate model not being constrained by observations. Oxygen concentrations are too low in both simulations, with shelf-mean whole-water column biases of −0.6 mg l^{-1} (hindcast) and −0.5 mg l^{-1} (RCP8.5).

To assess the oxygen concentrations, a WOD climatology was generated by binning observations for 1980 to 2009 onto the model grid and averaging according to the month of year. Regional averages of the hindcast near bed oxygen concentrations show similar seasonal variations as the WOD climatology (Fig. 2), although modelled oxygen concentration are generally too low and the minimum oxygen concentration occurs generally later in the year. The climatology of near bed oxygen from the RCP8.5 RP is similar to the hindcast in most regions; largest differences are in the more coastally dominated regions of the southern North Sea, English Channel, Skagerrak/Kattegat, Irish Sea and Armorican Shelf. For the shelf region, the mean difference in near-bed oxygen concentrations between the WOD climatology and the RCP8.5 simulation in the RP is 0.31 mg l^{-1}, for the hindcast the difference is 0.30 mg l^{-1}. We correct the biases in the hindcast and RCP8.5 near bed oxygen concentrations by adding 0.30 mg l^{-1} and 0.31 mg l^{-1}, respectively, to the simulated concentrations. For RCP8.5 we assume that the bias does not change during the simulation.

The impact of model drift is assessed by comparing time series of regional averages of the RCP8.5 and CTL simulations. Ideally, over the 120-year simulation, each year of the CTL simulation would be identical, with annual means of all variables constant. In practice, however, we expect that the CTL simulation will vary over time.

In the CTL simulation, regional averages of sea surface and near bed temperature and salinity (Figs. 3 and 4) have no significant trends (Appendix A.2). Trends in regional averages of near bed oxygen concentrations in CTL (Fig. 5) are significant (95% confidence) in many regions. However, except in the Celtic Sea and Armorican Shelf, the trends are at least an order of magnitude smaller than those of RCP8.5 (Appendix A.2). Since the changes in CTL are small compared to those in the RCP8.5 simulation, we consider that the spin up time for the RCP8.5 simulation is sufficiently long, that the simulation is not unduly influenced by model drift and changes are due primarily to the evolving atmospheric and oceanic forcing. Since the hindcast simulation had the same spin up length as CTL we assess that the hindcast is also sufficiently spun up from initial conditions. In all regions the CTL oxygen trend has opposite sign to the RCP8.5 trend, indicating that RCP8.5 might underestimate the impact of climate-forced changes.

4. Results

4.1. Projected changes to 2100

Averaged over regions of the NWES, near bed and surface temperature and salinity and near bed oxygen concentrations all show significant trends from 1980 to 2100 (Figs. 3–5): the NWES becomes fresher and warmer and near bed oxygen declines with time. The average regional warming over the 21st century of between 1.5 and 4.0 °C in NBT and between 2.7 and 4.0 °C in SST is similar to other modelling studies of the European shelf. [Tinker et al., 2016] calculate shelf-wide increases of 2.71 ± 0.75 °C and 2.90 ± 0.82 °C respectively from their model ensemble under the SRES A1B medium emissions scenario, which is less severe than the RCP8.5 scenario used here. Also under the A1B scenario, [Holt et al., 2010] calculate SST increases of 1.4–4.0 °C for the European Shelf and [Gröger et al., 2013] calculate SST warming of 1.6–3.2 °C on the European Shelf and 2 °C in the North Sea. The change of −0.7 to −1.9 in NBS compares to published estimates for the European shelf of −0.33 ± 0.38 [Tinker et al., 2016]. The SSS changes of −0.9 to −2.8 are also larger than published values of −0.41 ± 0.47 [Tinker et al., 2016], −0.2 [Holt et al., 2010] and −0.75 [Gröger et al., 2013]. [Gröger et al., 2013] attribute the freshening in their model to a combination of an intensifying hydrological cycle reducing salinity in the North Atlantic and an increase in freshwater run off from land. In our model, the freshening of Atlantic water affects much of the shelf and the impact is intensified by circulation changes in the North Sea, where a shutdown in Atlantic exchange leads to reduced circulation and decreased freshwater flushing from the North Sea [Holt et al., 2018].

The duration of seasonal stratification progressively increases over the NWES and adjacent Atlantic (Fig. 6a-d) in the near future (NF, 2025–2054) and far future (FF, 2070–2099) compared to the RP. By the FF, most of the North Sea is stratified for an additional month per year compared to the RP and the open Atlantic is stratified for an extra two months each year. The stratification also becomes stronger in the future with the open ocean, the shelf edges, the Celtic Sea and the eastern and northern North Sea being most affected (Fig. 6e-h).

By the end of the 21st century, net primary production (netPP) increases in all areas except for the western and central North Sea and the outer shelf regions north and west of Scotland and Ireland (Fig. 7b). The change in netPP largely reflects the change in dissolved inorganic nitrogen [Holt et al., 2018]. The FF increase in the strength of stratification in the off-shelf region inhibits the mixing of nutrients from below the pycnocline and decreases the nutrient supply to surface waters. This contributes to a reduction in netPP in the open Atlantic and in shelf regions affected by on-shelf nutrient transport (the Irish and Scottish shelves and the western North Sea). In the RCP8.5 simulation, a decrease in the North Sea circulation in the 2040 s ([Holt et al., 2018]) increases the retention time of riverine water in the North Sea and leads to an increase in winter nutrient concentrations in the eastern North Sea and Norwegian Trench even though river nutrient sources are held at present day values. This fuels an increase in netPP. NetPP also increases in the Irish Sea, Celtic Sea and the western English Channel due to an increase in winter nutrient concentrations. A regional POLCOMS-ERSEM simulation under the SRES A1B medium emissions scenario [Holt et al., 2012] shows that nutrient availability is a major control on primary production which, by the end of the 21st century, leads to

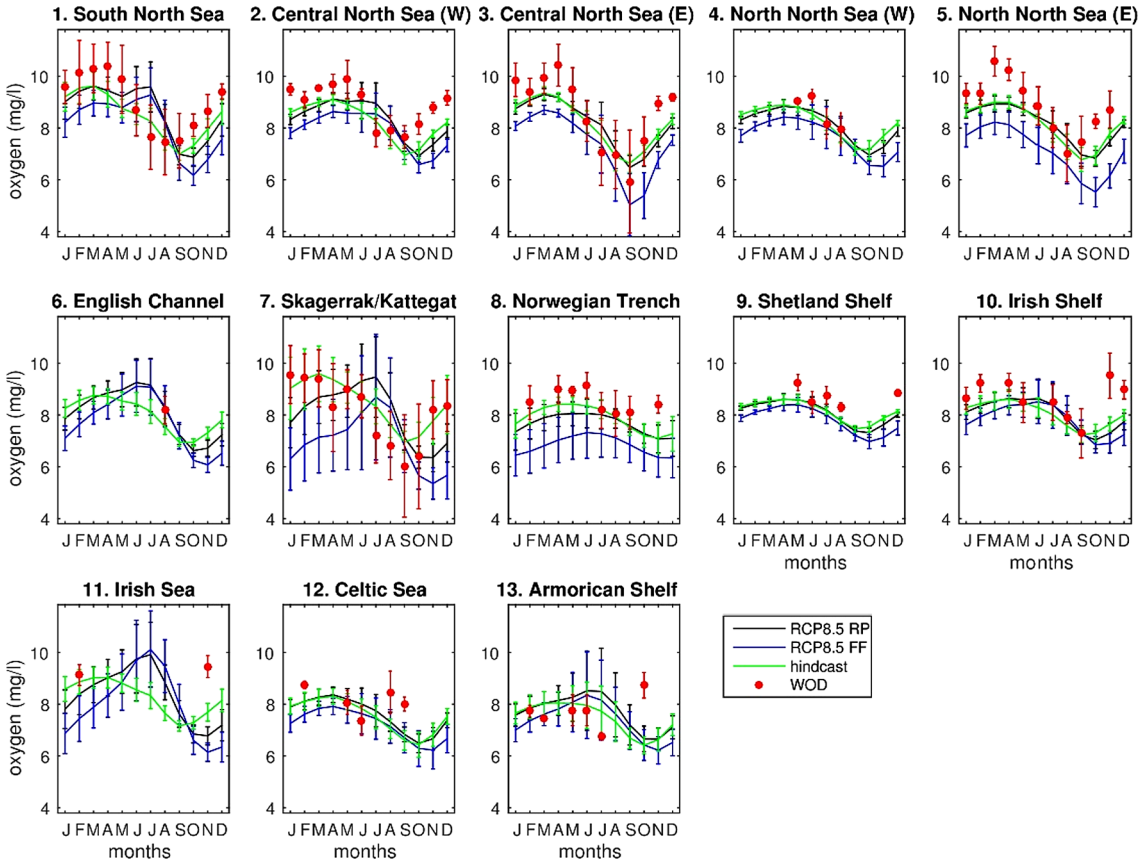

Fig. 2. Mean annual signal of near bed oxygen averaged over the 13 regions shown in Fig. 1 from the RCP8.5 simulation recent past (RP, 1980–2009) and far future (FF, 2070–2099), the hindcast simulation and the climatology derived from the World Ocean Database (WOD) observations. Error bars are one standard deviation of the monthly-mean climatologies in each region.

reduced netPP in the open ocean and the northern North Sea and higher netPP elsewhere on the NWES. In a global MPIOM-HAMOCC simulation under the A1B scenario [Gröger et al., 2013] finds a strong decline (~30%) in the productivity of the whole NWES by 2100 due to reduced nutrient supply from the deep Atlantic.

Bacterial respiration is the main process that consumes oxygen near the sea bed. Respiration rates are higher in coastal regions and in the southern half of the North Sea and reduce towards the open ocean (Fig. 7c). By the end of the 21st century (Fig. 7d), respiration has increased everywhere except for the Norwegian Trench, along the whole shelf edge and in the western North Sea. Changes between FF and RP mirror spatially those of netPP except for in the Norwegian Trench where bacterial respiration is reducing even though netPP increases, and west of Denmark where respiration increases despite a weak reduction in netPP. The Norwegian Trench is a deep and highly advective region so we would not necessarily expect the change in surface netPP to be reflected in the near bed bacterial respiration. West of Denmark there is a reduction in the strength of the southern North Sea current ([Holt et al., 2018]), so that a larger proportion of detritus produced in this region reaches the sea bed, offsetting the decrease in netPP.

We define the time of emergence of the climate change signal from average RP conditions as the mid-year of a 30-year period where the 30-year mean differs from the 1980–2009 mean by more than twice the standard deviation of the 1980–2009 annual means. In all regions except for the English Channel and the Irish and Celtic Seas, salinity is the first to differ from the RP (Fig. 8). In general, the SST change emerges before the NBT change. Except for in the eastern North Sea, the Skagerrak/Kattegat and Norwegian Trench, near-bed oxygen change emerges later than that of temperature and salinity; on the Shetland shelf, oxygen change emerges at the same time as NBT change. Years of the emergence of annual mean oxygen change vary from 2033 in the Norwegian Trench to 2072 on the Irish shelf. The generally later emergence of the climate change signal in near-bed oxygen concentrations could be due to larger interannual oxygen variability or might indicate that other factors (e.g. ecosystem processes) mitigate temperature and salinity impacts on oxygen concentrations.

In addition to trends in annual mean oxygen, the seasonality of the oxygen cycle also changes. Near bed oxygen in the FF is generally lower throughout the year than in the RP (Fig. 2) but the amplitude and timing of the seasonal cycle changes. In general, the amplitude change corresponds to the change in netPP (Fig. 7); regions with reduced or small increases in netPP have reduced amplitudes while regions with larger increases in netPP have increased amplitudes. In the western Central North Sea and the Celtic Sea the amplitude reduces by 7–10% in the FF compared to RP. In all other regions, except for the Norwegian Trench, the amplitude of the seasonal cycle increases in the FF, with amplitudes in the Irish Sea and eastern Central and northern North Sea increasing by more than 25%. The month of minimum oxygen concentration changes in the western northern North Sea, the English Channel and the Celtic Sea from October in the RP to November in the FF. Between the RP and FF, the peak regional mean SST and NBT (not shown) also occur later in the year. This affects oxygen solubility, which contributes to the delay in the month of minimum oxygen in the FF.

4.2. Minimum near bed oxygen

Near bed oxygen minimum concentrations that fall below healthy values, especially where such conditions persist, can be damaging to the ecosystem. Monthly mean oxygen concentrations output from the

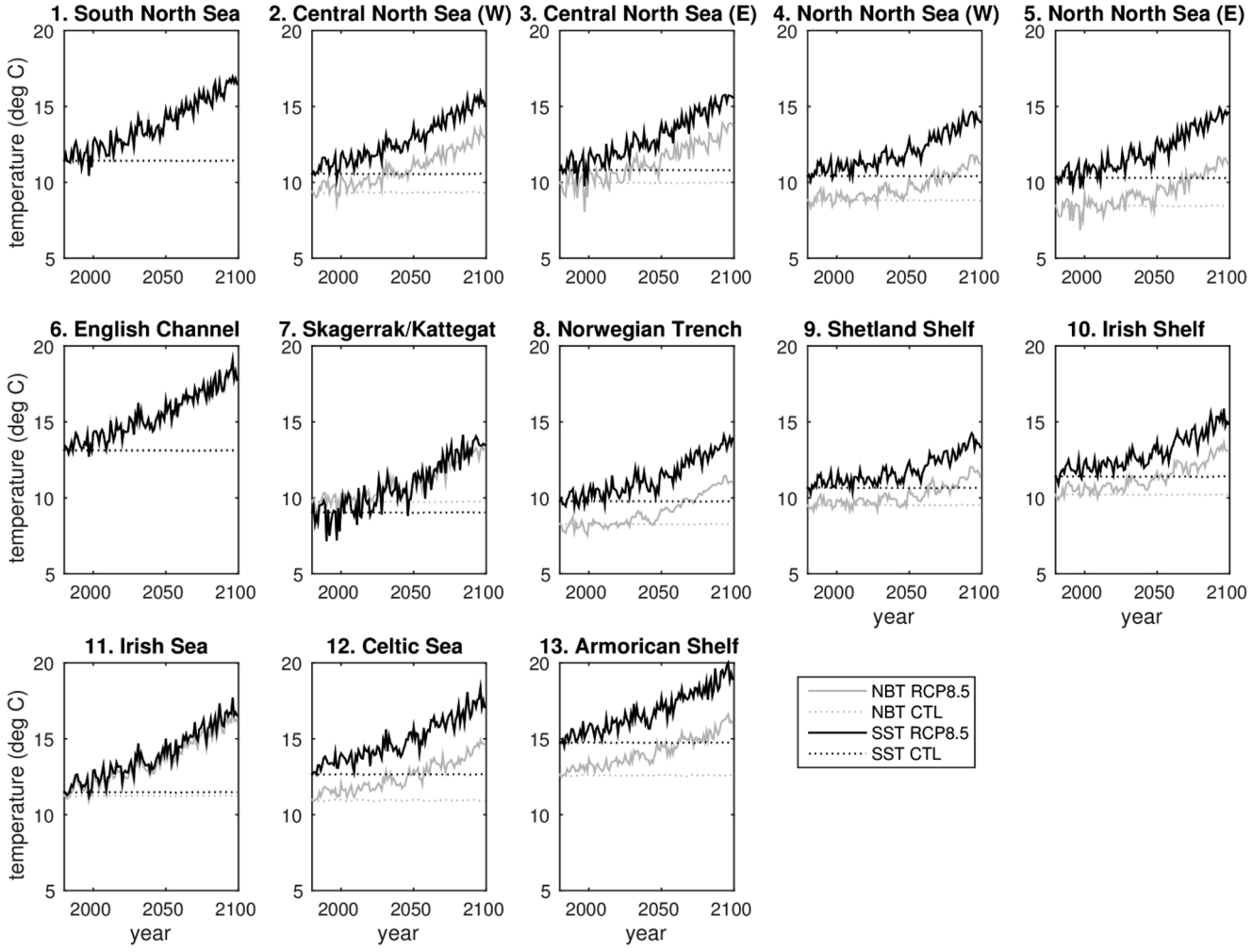

Fig. 3. Time series of annual mean near bed temperature (NBT) and sea surface temperature (SST) averaged over shelf regions (Fig. 1) for the RCP8.5 and CTL simulations.

NEMO-ERSEM simulations are not suitable for studying short periods of oxygen depletion but can be used to study the spread of low-oxygen areas and changes in the duration and frequency of low-oxygen episodes.

The hindcast shows a broad area in the eastern North Sea where minimum monthly-mean oxygen concentrations below 5 mg l^{-1} occurred during 1980–2007 (Fig. 9a), with regions west to east at 55–57°N through the central North Sea, in the Celtic Sea, Armorican Shelf and Norwegian Trench experiencing values less than 6 mg l^{-1}. Minimum oxygen concentrations for the RCP8.5 RP (Fig. 9b) are slightly higher but show the same regions of oxygen depletion as the hindcast, with similar minimum concentrations. In a decadal (1998 to 2009) reanalysis of the NWES [Ciavatta et al., 2016] show large areas vulnerable to near-bed oxygen deficiency. They identify the same regions of low oxygen concentrations in the recent past as in this study, namely, the eastern North Sea, the Celtic Sea and Armorican shelf. However, using the definition of vulnerability to be a day with mean concentration falling below 6 mg l^{-1}, they additionally identify potential oxygen depletion areas to the west of Ireland, in coastal zones of Scotland and in the eastern English Channel.

In the near future (2025 to 2054, Fig. 9c), the region in the eastern North Sea with minimum oxygen below 5 mg l^{-1} grows and includes a region below 4 mg l^{-1} while the area with 6 mg l^{-1} and below has extended into the Irish Sea and English Channel. By the end of the century (Fig. 9d), minimum oxygen in the eastern North Sea is widely below 2 mg l^{-1}, and only coastal areas, the outer shelf regions and the western North Sea are above 6 mg l^{-1}.

To study the evolution of regions with low oxygen concentrations we define a threshold O2T = 6 mg l^{-1} using the "oxygen depletion" concentration for the North Sea [OSPAR, 2003]. In more than 40% of years in the hindcast and RCP8.5 RP simulations, regions of the eastern North Sea, Celtic Sea and Armorican shelf experience at least one month with mean oxygen concentrations below the threshold (Fig. 9e,f). In the Skagerrak/Kattegat and the southern Norwegian Trench, values are below the threshold for more than 20% of years in the RCP8.5 RP simulation. By the NF (Fig. 9g), more than 60% of years are below the threshold in the eastern North Sea, Celtic Sea and southern Norwegian Trench and, by the end of the century (Fig. 9h), large parts of these areas go below the threshold in more than 80% of years. By the same time, parts of the Armorican shelf have concentrations below the threshold in more than 80% of years and the Irish Sea and English Channel have regions with low oxygen in more than 40% of years. By 2100, minimum oxygen concentrations in the western English Channel, Irish and Shetland shelves and the western North Sea remain above the threshold (Fig. 9m); regions of low oxygen concentration spread north-westward in the North Sea with time, and north-eastwards and south-eastwards in the Celtic Sea. The average number of months each year affected by low oxygen concentrations is small in the RP (Fig. 9i,j), the eastern North Sea is most affected but in less than one month every two years. By the 2025–2054 NF period, oxygen is low in the eastern North Sea for up to two months per year on average (Fig. 9k) and, by the FF (Fig. 9l), more than four months per year. In the

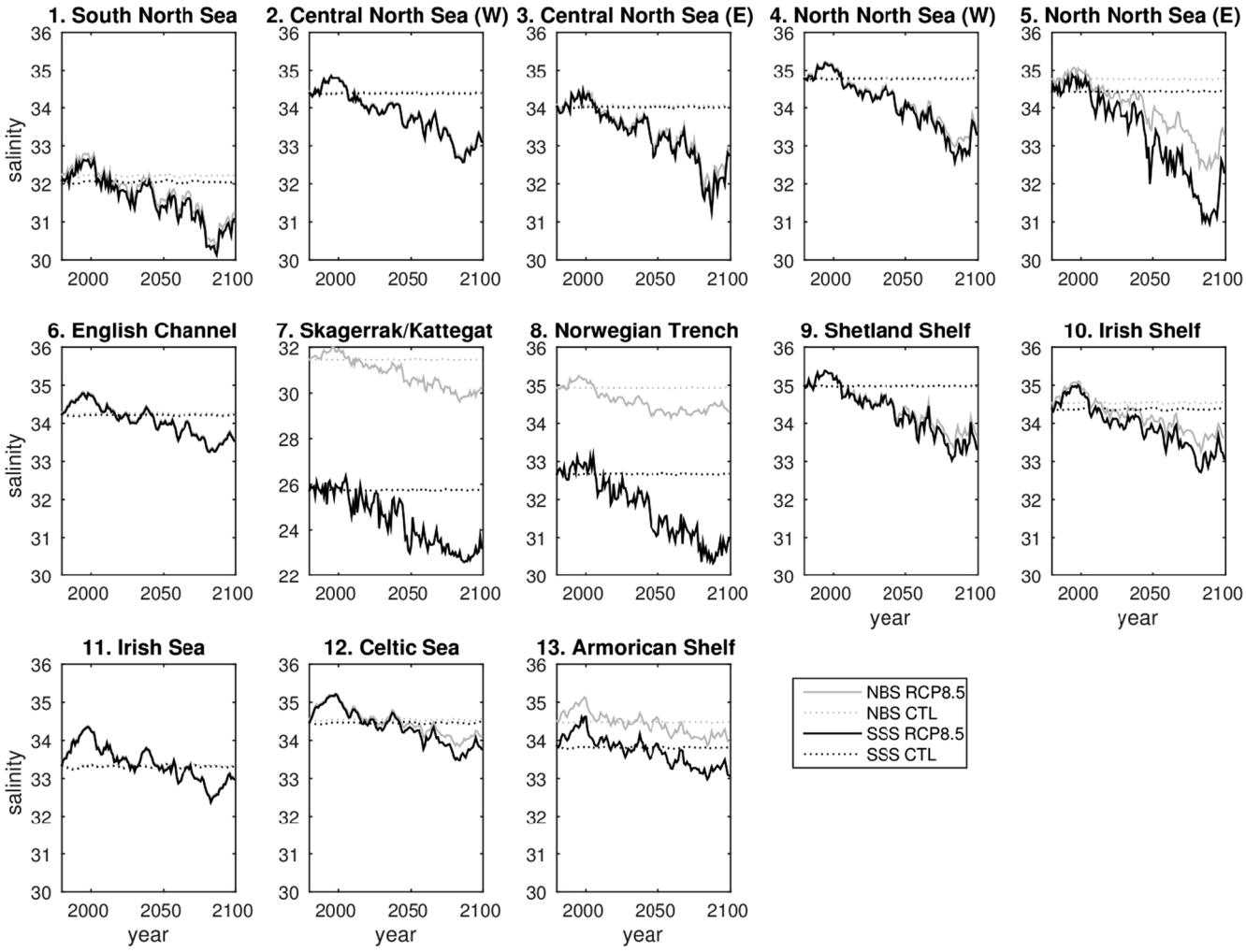

Fig. 4. Time series of annual mean near bed salinity (NBS) and sea surface salinity (SSS) averaged over shelf regions (Fig. 1) for the RCP8.5 and CTL simulations.

Celtic Sea and Armorican shelf, oxygen is low in up to one month every two years in the NF and up to twice as long in the FF. The area of the NWES with oxygen below the threshold concentration increases by ~240% between the RP and the FF.

4.3. Controls on near bed oxygen

All regions experience the same general temperature and salinity trends from 1980 to 2100, with the climate becoming warmer (Fig. 3) and fresher (Fig. 4). The impact of warming dominates over that of decreasing salinity and the effect of the temperature/salinity changes is to reduce oxygen concentrations in all shelf regions by 2100 (Fig. 10). By the end of the century, the average reduction in annual oxygen concentration from solubility changes ranges from 0.20 ± 0.09 mg l^{-1} on the Shetland shelf to 0.60 ± 0.10 mg l^{-1} in the southern North Sea (Table 2). Differences in oxygen concentration between FF and RP time slices (Fig. 11b) show that the impacts are smaller near the shelf edge coinciding with deeper areas where temperature increases are smaller (Fig. 12a). The freshening of the shelf (Fig. 12b) acts to increase oxygen solubility and mitigates the impact of increasing temperature particularly in the North Sea where the reduction in salinity is strongest. The relative impacts of the temperature and salinity changes are estimated by calculating the change in oxygen solubility [Weiss, 1970] due to the change in temperature/salinity with the salinity/temperature at constant RP values (Fig. 12e,f). On average the magnitude of the salinity effect is ~20% of the temperature effect, ranging from < 10% in the Norwegian Trench to > 30% north and northwest of Scotland.

During the month of minimum oxygen concentration, the impact of temperature/salinity changes ($\Delta DO_p^{\min}$, Fig. 13) is less than for the annual mean and varies between 0.11 ± 0.09 mg l^{-1} on the Shetland Shelf and 0.54 ± 0.06 mg l^{-1} in the southern North Sea (Table 2). There is little seasonal signal in the salinity change between FF and RP (Fig. 12b,d). However, the temperature change in the month of minimum oxygen (Fig. 12c) is more spatially variable than the annual signal (Fig. 12a) with larger increases in the southern North Sea, Irish Sea and English Channel, and smaller increases in the western Northern North Sea and the Shetland and Irish Shelves. On most of the shelf, the changes act to reduce the oxygen concentration. However, in parts of the eastern Central North Sea, the temperature in the month of minimum oxygen concentration (mostly September in this region, Fig. 12i) is actually decreasing into the future (Fig. 12c), while the salinity also falls. Thus the physical driver is increasing oxygen concentrations here (Fig. 11g). There is also an increase in oxygen concentrations in the region of weak warming east of Scotland. The salinity effect is on average ~20% of the temperature effect (Fig. 12g,h) but exceeds the impact of temperature in regions of small temperature changes.

In many regions, the impact on oxygen concentrations of changing the solubility is larger than the ecosystem impact (Fig. 10 and Fig. 13). By about 2030 in the Skagerrak/Kattegat and Norwegian Trench, and from 2050 onwards in the eastern Central North Sea and the Northern North Sea, changes to ecosystem processes act to reduce both annual mean and annual minimum oxygen concentrations. At the end of the century, in the eastern Northern North Sea, Skagerrak/Kattegat and

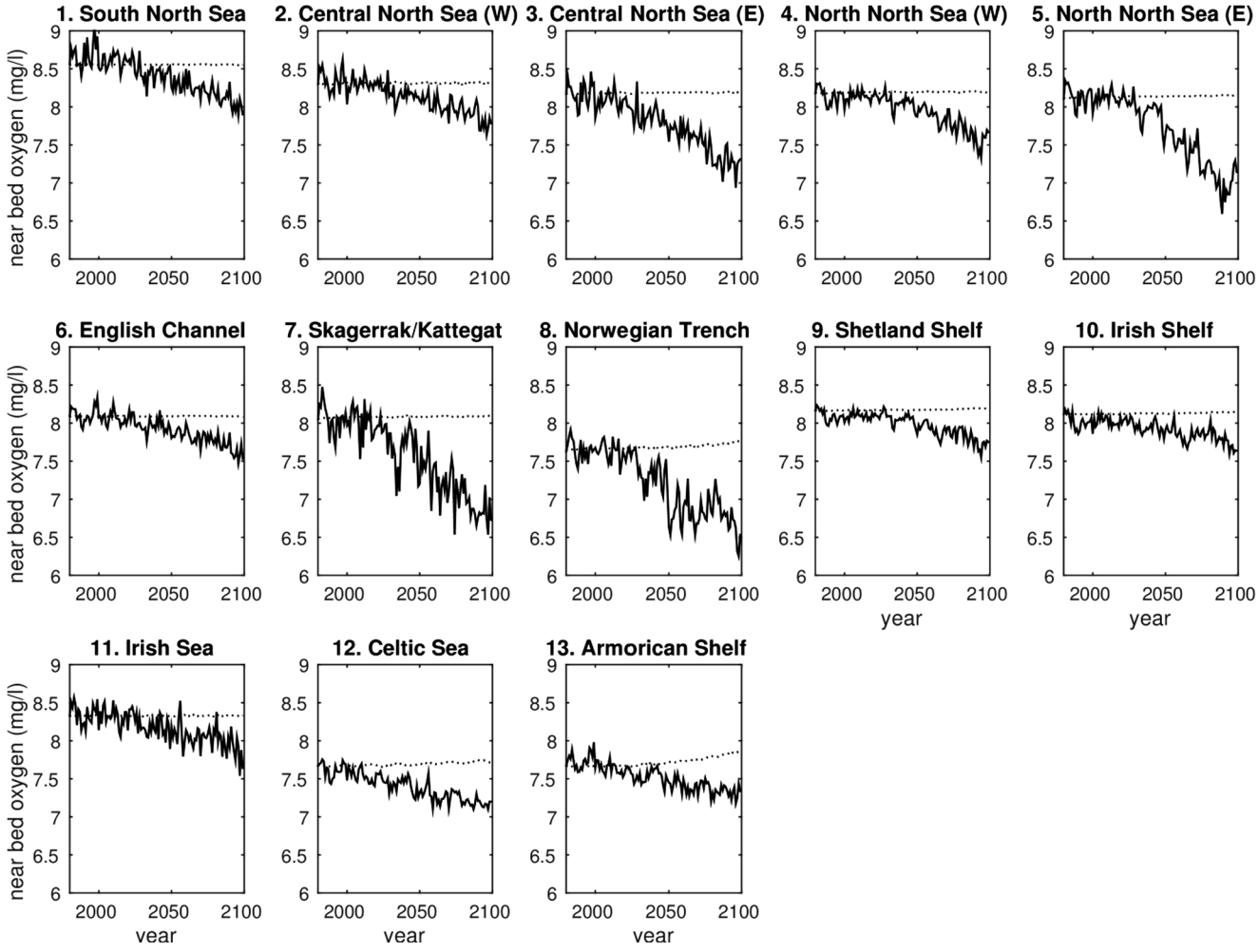

Fig. 5. Time series of annual mean near bed oxygen concentrations averaged over shelf regions (Fig. 1). The solid line is the RCP8.5 simulation and the dotted line is the CTL run.

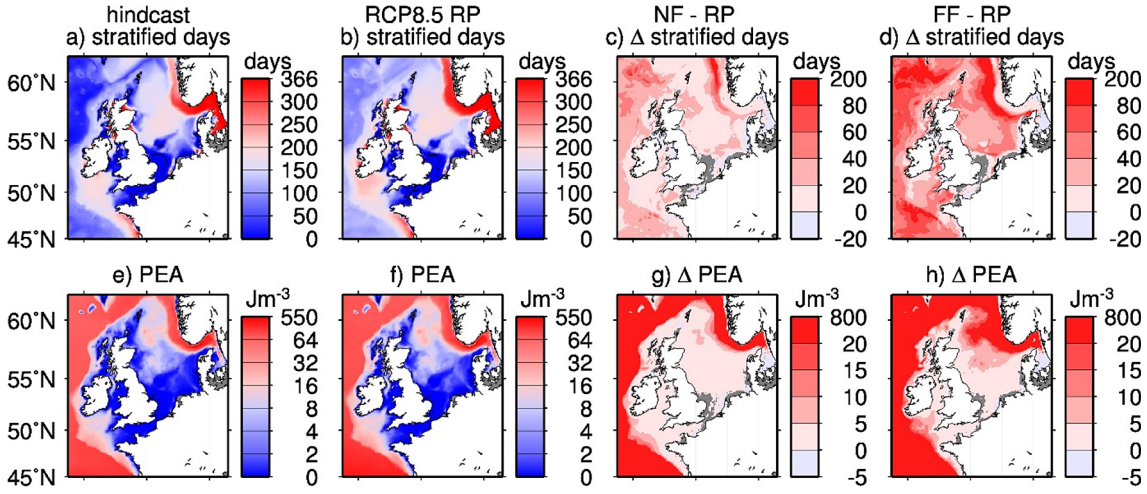

Fig. 6. Average number of seasonally stratified days (with surface to bottom density difference greater than that equivalent to a 0.5 ˚C temperature decrease, and a surface mixed layer shallower than 50 m) and the average potential energy anomaly (PEA, the energy required to mix the water column from the surface to the bed or 400 m depth) for the hindcast (column 1) and the RCP8.5 recent past (RP, 1980–2009) simulation (column 2). Also shown (column 3) is the change between the RCP8.5 near future (NF, 2025–2054) and RP and (column 4) the change between RCP8.5 far future (FF, 2070–2099) and RP.

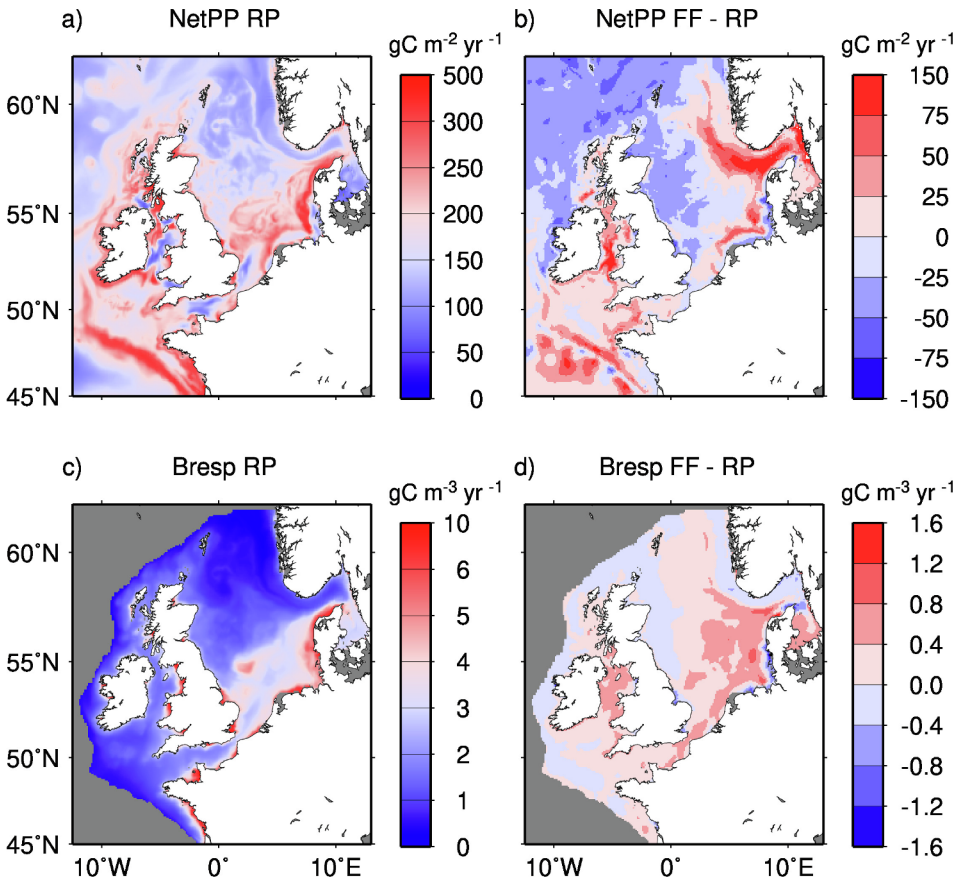

Fig. 7. Depth integrated mean annual net primary production from a) the RCP8.5 recent past (RP, 1980–2009) simulation and b) the difference between the RCP8.5 far future (FF, 2070–2099) and RP; mean near bed bacterial respiration (shelf only) in c) the RP and d) the difference between FF and RP.

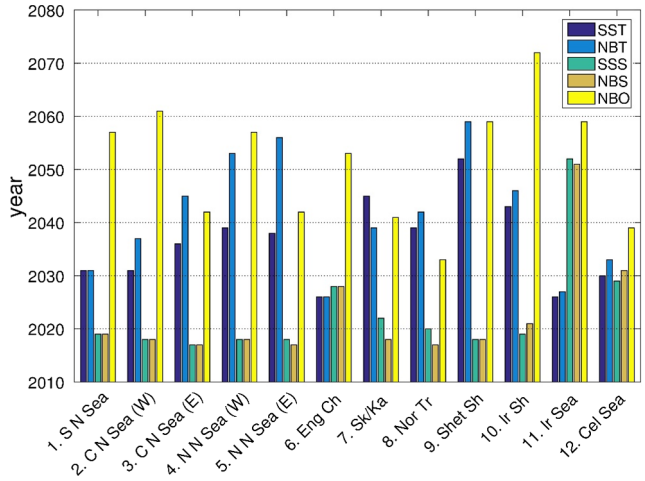

Fig. 8. Time of emergence of the climate change signal compared to the 1980 to 2009 period for sea surface (SST) and near bed (NBT) temperature, sea surface (SSS) and near bed (NBS) salinity, and near bed oxygen concentrations (NBO) from annual means averaged over shelf regions (Fig. 3-Fig. 5).

Norwegian Trench, the ecosystem effect is larger than the solubility one, with annual reductions of 0.48 ± 0.21 to 0.70 ± 0.20 mg l^{-1} (Table 2). In the eastern parts of the central and Northern North Sea, the oxygen reduction due to ecosystem processes in the month of minimum oxygen (1.21 ± 0.51 and 1.05 ± 0.36 mg l^{-1}, respectively) is particularly strong and is 77% and 61%, respectively, of the total change. In the Southern North Sea, English Channel, Irish Shelf and Irish Sea, changes in ecosystem processes mitigate oxygen reductions due to solubility changes and annual mean oxygen concentrations by the end of the century are higher than are projected from solubility changes alone. However, ecosystem processes act to reduce minimum oxygen concentrations in all regions except for the Irish Shelf.

The ecosystem contribution to oxygen change by the FF (Fig. 11 d, h) is particularly strong in the eastern North Sea and the Skagerrak and acts to decrease both annual and minimum near bed oxygen. In the eastern North Sea, the water is cooling in the month of minimum oxygen concentration (Fig. 12c), while the salinity also falls. Thus, the solubility change (Fig. 11g) is increasing oxygen concentrations here while ecosystem processes (Fig. 11h) act to reduce it.

Decreasing oxygen concentrations on the Shetland and Irish shelves are primarily due primarily to changes in the temperature/salinity climate (Fig. 11). Near the shelf edge west of Ireland, in the Celtic Sea and on the northern part of the Armorican Shelf, oxygen concentration increases due to ecosystem changes.

Changes in minimum oxygen concentrations (Fig. 13) are a lower bound on the actual changes since the month of minimum oxygen altered during the RCP8.5 simulation, occurring later in the year by the end of the 21st century (Fig. 12j). Thus oxygen decreases are likely to be underestimated and oxygen increases to be overestimated.

Averaged over the shelf the projected change in mean (minimum) oxygen concentrations by the FF compared to the RP is 6.3% (7.7%) of which the solubility component is 73% (50%) of the total.

4.4. Biogeochemical controls on near bed oxygen

Minimum monthly oxygen concentrations in the RP (Fig. 11e) reflect the spatial distribution of netPP (Fig. 7a), being generally lower in the southern and eastern NWES where netPP is higher, and higher in the northern North Sea, in the Norwegian Trench and North of Scotland

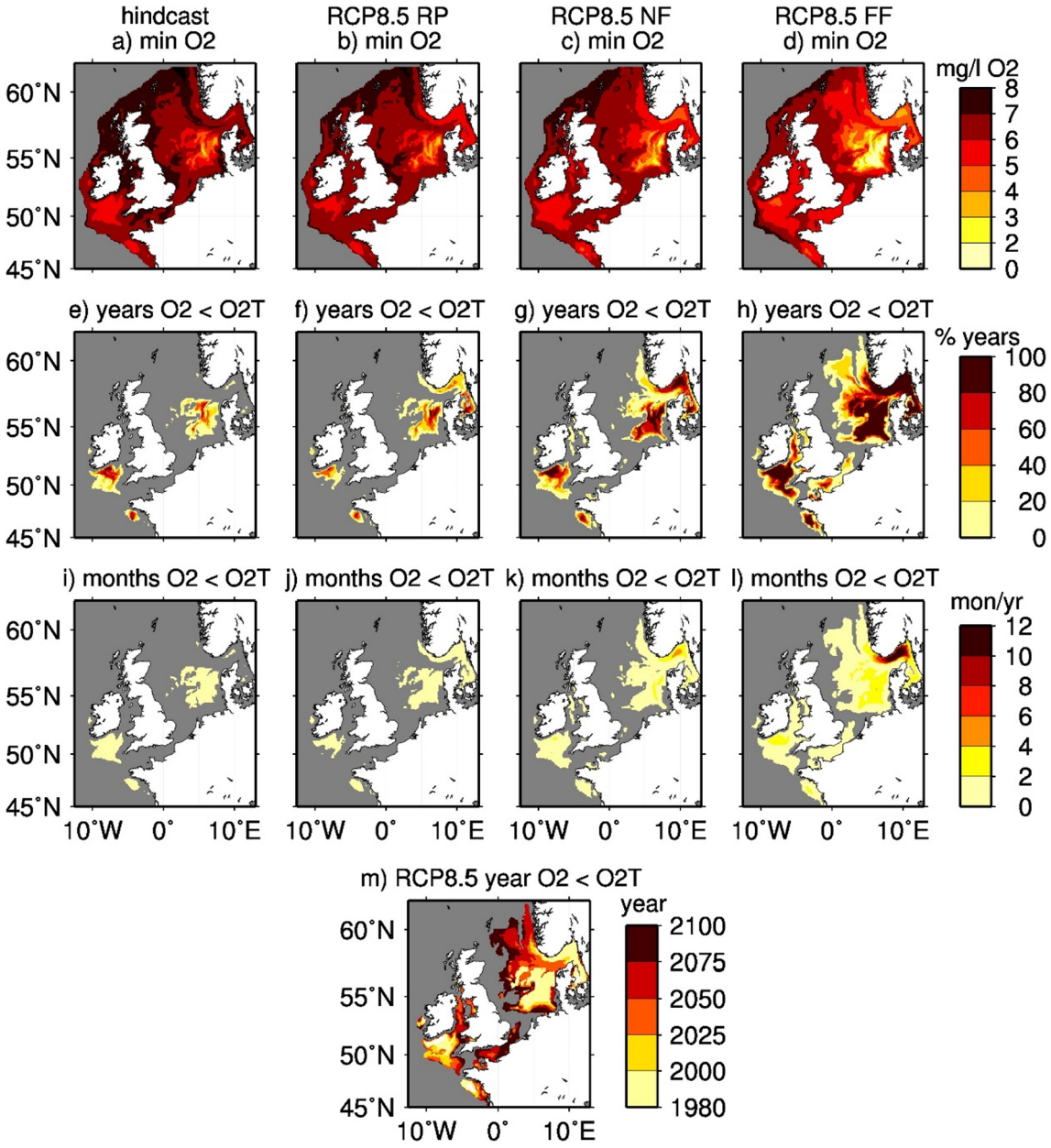

Fig. 9. Bias-corrected near bed oxygen: hindcast simulation in column 1; RCP8.5 recent past (RP, 1980–2009) in column 2; RCP8.5 near future (NF, 2025–2054) in column 3 and RCP8.5 far future (FF, 2070–2099) in column 4. a) – d) Minimum monthly mean near bed oxygen during the simulation periods. e) – h) Percentage of years during each period when monthly mean near bed oxygen falls below the threshold concentration O2T. i) – l) Average duration of monthly mean near bed oxygen below O2T. m) First year when monthly mean near bed oxygen in the RCP8.5 simulation falls below O2T. Off-shelf regions and regions in e) – m) where the threshold concentration is not reached are coloured grey.

where netPP is lower. The FF increase in netPP (Fig. 7b) prompts a general decrease in near-bed oxygen concentrations (Fig. 11 d, h). An estimate of the net phytoplankton growth contributing to oxygen change in the water column is calculated for each year by integrating the netPP from January (when the water column is well-mixed on the shelf and oxygen concentrations are in near-equilibrium with the atmosphere) to the month of minimum oxygen. To suppress the climate change signal that would otherwise dominate correlation statistics, a linear trend is removed from the time series. The change in minimum oxygen due to ecosystem changes (ΔDO_e^{min})is negatively correlated (at 99% significance) with this seasonal netPP (Fig. 14a) over much of the NWES. However, there is no significant correlation in the Southern Bight of the North Sea, the Irish Sea and near the shelf edge in the Celtic Sea and Armorican Shelf.

Whilst netPP is at the start of the chain of ecosystem processes affecting oxygen in the water column, other processes, such as transport and mixing of organisms, mean that regions of maximum phytoplankton growth in the top of the water column (where sun light penetrates and fuels primary production) are not necessarily where lowest near-bed oxygen concentrations occur. This is particularly true near the shelf edge where there is exchange with the deeper North Atlantic and in the Norwegian Trench where there is strong advection.

ΔDO_e^{min} correlates negatively with near-bed bacterial respiration (integrated from January to the month of minimum oxygen) everywhere on the NWES except for isolated regions and between Northern Ireland and Scotland where the correlation is not significant (Fig. 14b). Regions of decreasing/increasing respiration (Fig. 7d) correspond to areas where the ecosystem change acts to increase/decrease oxygen concentrations (Fig. 11h); there is also a clear contrast in the respiration change between the western and eastern North Sea that mirrors the

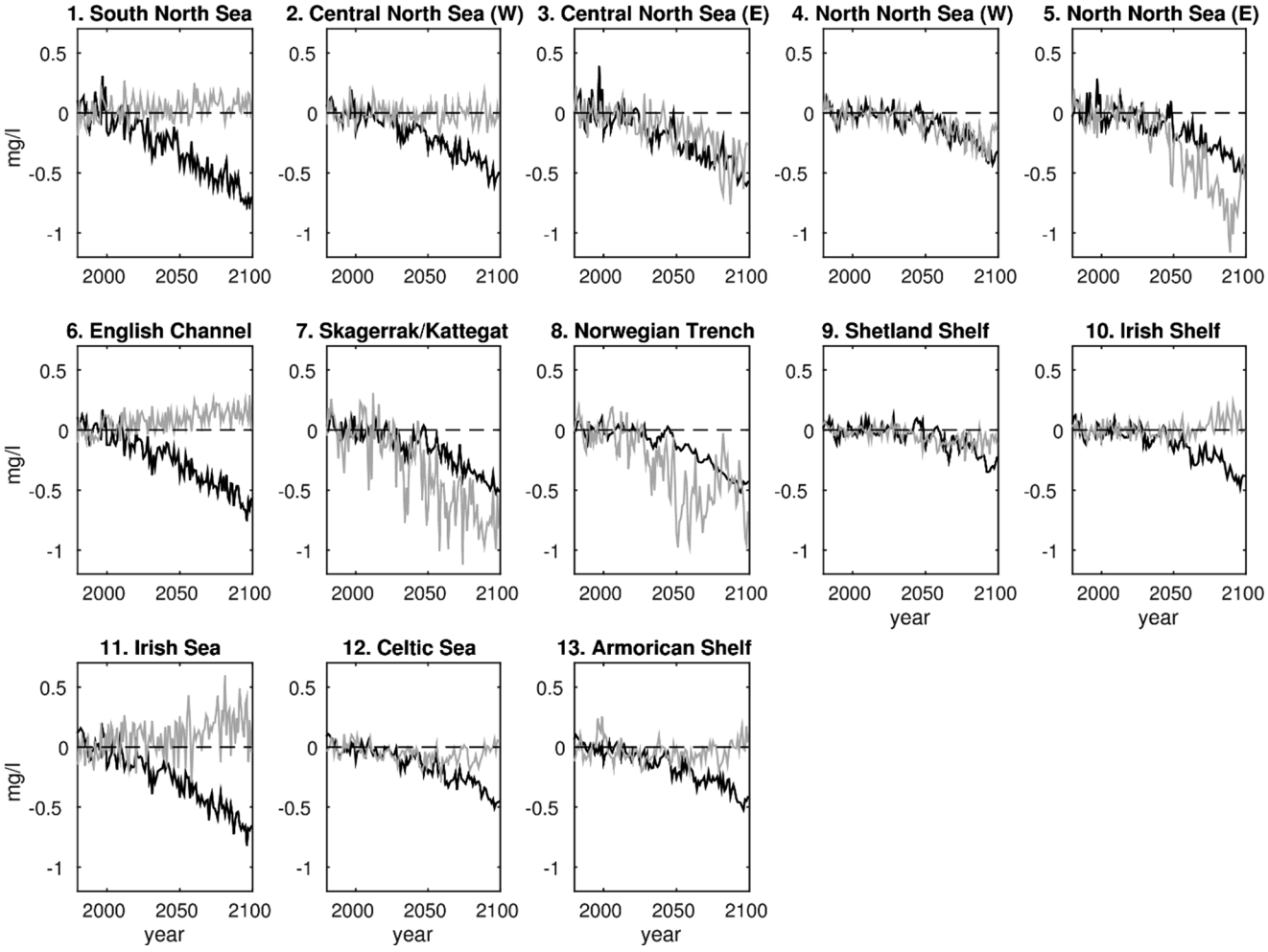

Fig. 10. Changes relative to the RP of the annual mean near bed oxygen (from Fig. 5) due to temperature/salinity changes (ΔDO_p^{ann}, black line) and evolving ecosystem processes (ΔDO_e^{ann}, grey line) for the 13 regions defined in Fig. 1.

ecosystem impact. In the regions where the ecosystem impact on oxygen is largest, increasing netPP in the future leads to larger accumulation of particulate detritus near bed, fuelling bacterial respiration.

Near-bed phytoplankton and zooplankton respiration do not have the same coherent shelf-wide correlations with ΔDO_e^{min} (not shown) as bacterial respiration and are not such primary controls on near-bed minimum oxygen concentration. In regions where oxygen depletion is apparent, phytoplankton and zooplankton respiration are positively correlated with oxygen concentrations. Away from regions prone to oxygen depletion, zooplankton and phytoplankton respiration, similar to bacterial respiration, correlate negatively with ΔDO_e^{min}, that is, there is a straightforward relation with more respiration consuming more oxygen.

Stratification is important for oxygen dynamics in regulating primary production through controlling nutrient supply and in isolating near-bed waters from gas-exchange with the atmosphere. In the stratified regions, generally ΔDO_e^{min} is correlated to both the duration of stratification and the strength (PEA) in the month of minimum oxygen (Fig. 14 c, d). However, there is no significant correlation with stratification strength in much of the Celtic Sea where stratification is possibly always sufficiently strong to isolate bottom waters, although the duration of stratification is significantly correlated here. The strongest correlation with stratification strength is in the area that experiences oxygen depletion south of Dogger Bank in the North Sea.

In isolated regions of the shelf, ΔDO_e^{min} is positively correlated with netPP and the strength and duration of stratification (Fig. 14). In the more dynamic environments: the Norwegian Trench, near the shelf edge and in frontal regions between areas that seasonally stratify and areas that remain vertically mixed, local mixing and transport processes disrupt the relationship between ΔDO_e^{min} and netPP and stratification.

5. Summary and conclusions

We used the coupled physics-biogeochemical model NEMO-ERSEM to study the evolution to 2100 of near-bed oxygen concentrations for the Northwest European Continental shelf under a high greenhouse gas emissions scenario (RCP8.5). Comparisons with a hindcast simulation confirm that the recent past climate of the RCP8.5 simulation gives a reasonable estimate of temperature, salinity and near-bed oxygen climates. A combination of time series of regional averages and time-slice maps were used to study both time evolution and spatial patterns of change. While the responses to climate change on the shelf are generally coherent (warming, freshening and decreasing near-bed dissolved oxygen), the oxygen change is a combination of responses to

Table 2
Change in near bed oxygen concentration from 1980–2009 to 2070–2090 due to temperature/salinity changes (ΔDO_p^{ann}, ΔDO_p^{min}) and evolving ecosystem processes (ΔDO_e^{ann}, ΔDO_e^{min}) for the 13 regions defined in Fig. 1. All changes except for those in grey are different from zero with 95% confidence, determined using a one-sample *t*-test. The variability of the changes is given by ± their standard deviation during 2070–2090.

Region	hydrodynamic impact (mg l^{-1})		ecosystem impact (mg l^{-1})	
	ΔDO_p^{ann}	ΔDO_p^{min}	ΔDO_e^{ann}	ΔDO_e^{min}
1. South North Sea	-0.60 ± 0.10	-0.54 ± 0.06	0.07 ± 0.07	-0.07 ± 0.12
2. Central North Sea (W)	-0.42 ± 0.09	-0.33 ± 0.08	-0.01 ± 0.08	-0.03 ± 0.16
3. Central North Sea (E)	-0.43 ± 0.10	-0.17 ± 0.09	-0.37 ± 0.18	-1.21 ± 0.51
4. North North Sea (W)	-0.26 ± 0.09	-0.15 ± 0.08	-0.21 ± 0.10	-0.25 ± 0.16
5. North North Sea (E)	-0.35 ± 0.08	-0.17 ± 0.07	-0.66 ± 0.22	-1.05 ± 0.36
6. English Channel	-0.53 ± 0.10	-0.47 ± 0.08	0.14 ± 0.07	-0.01 ± 0.09
7. Skagerrak/Kattegat	-0.38 ± 0.09	-0.24 ± 0.06	-0.70 ± 0.20	-0.64 ± 0.22
8. Norwegian Trench	-0.38 ± 0.08	-0.27 ± 0.07	-0.48 ± 0.21	-0.41 ± 0.26
9. Shetland Shelf	-0.20 ± 0.09	-0.11 ± 0.09	-0.09 ± 0.07	-0.15 ± 0.13
10. Irish Shelf	-0.30 ± 0.10	-0.23 ± 0.09	0.07 ± 0.08	0.06 ± 0.09
11. Irish Sea	-0.57 ± 0.10	-0.51 ± 0.08	0.21 ± 0.17	-0.05 ± 0.15
12. Celtic Sea	-0.34 ± 0.09	-0.24 ± 0.07	-0.05 ± 0.07	0.01 ± 0.10
13. Armorican Shelf	-0.35 ± 0.09	-0.28 ± 0.07	-0.01 ± 0.09	-0.04 ± 0.10

temperature, salinity and ecosystem changes that varies over the shelf with large differences even within the sub-regions studied here. In most regions of the NWES, the climate change signal emerges first in salinity (generally before 2020), then in temperature and finally (between 2033 and 2072) in near bed oxygen concentrations.

Regions of the eastern North Sea, the Celtic Sea and the Armorican shelf were found to experience near-bed oxygen depletion in the recent past. Under the RCP8.5 scenario, these regions are projected to increase in size and to experience more sustained oxygen depletion periods by 2100. Other regions, namely the western North Sea, the western English Channel and shelf regions west and north of Scotland, are projected not to experience low oxygen concentrations. The seasonality of the oxygen cycle also changes, with the month of minimum oxygen generally occurring later in the year by 2100 than in the recent past.

Water temperature and salinity, oxygen replenishment from the atmosphere and ecosystem processes all affect dissolved oxygen. Under projected changes in temperature, salinity and ecosystem function there are complex competing (warming/freshening) and interacting (ecosystem and the physical climate) processes influencing oxygen concentrations. Using a coupled hydrodynamic-ecosystem model simulation, the impact of changing temperature and salinity has been decoupled from the impact of the evolving ecosystem so that the relative importance of solubility versus ecosystem processes can be assessed. The driving force behind the ecosystem change is netPP (controlled by nutrient availability) combined with seasonal stratification, which isolates sub-pycnocline waters from atmospheric exchange and also retains detritus in the lower part of the water column. For the NWES, the ecosystem component of near bed minimum oxygen correlates significantly on inter-annual (de-trended) timescales with netPP and the duration and strength of stratification. However, it is more widely correlated with near bed bacterial respiration, and this correlation extends into areas that are not affected by seasonal stratification. The correlation with bacterial respiration indicates that the derived ecosystem components of oxygen change (ΔDO_e^{ann}, ΔDO_e^{min}) represent the impacts of changes in the near bed ecosystem.

Until about 2040, the impact of solubility, generally acting to reduce near bed oxygen, dominates over the effects of the evolving ecosystem. After 2040, changes in the ecosystem in the eastern Northern

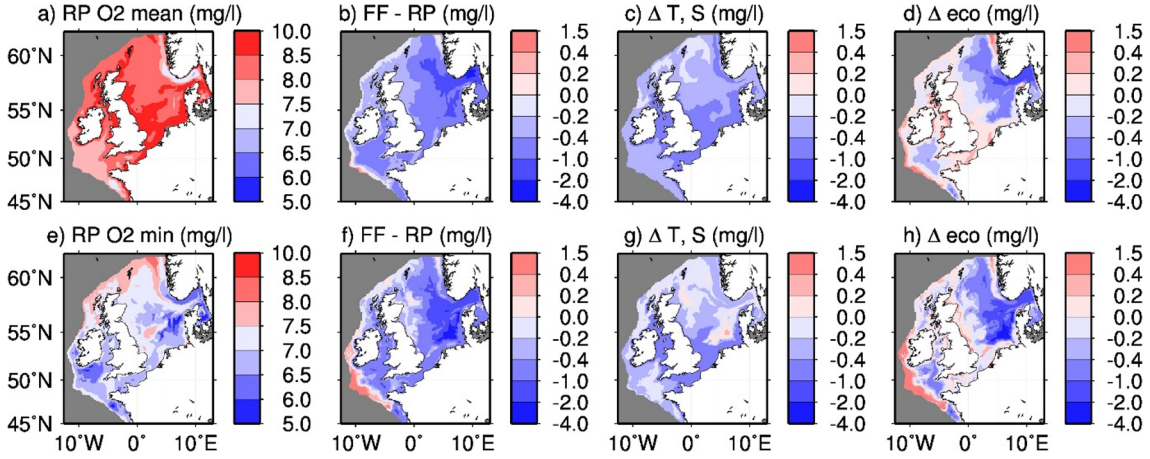

Fig. 11. Bias-corrected near bed oxygen concentration in the recent past (RP, 1980–2009) for a) annual mean and e) the monthly minimum. b) The change in annual and f) the change in monthly minimum near bed oxygen from the RP to the far future (FF, 2070–2099). c) The contribution of temperature/salinity changes ΔDO_p^{ann} to b), and d) the contribution of changes in the ecosystem ΔDO_e^{ann} to b). g) The contribution of temperature/salinity changes ΔDO_p^{min} to f), and h) the contribution of changes in the ecosystem ΔDO_e^{min} to f).

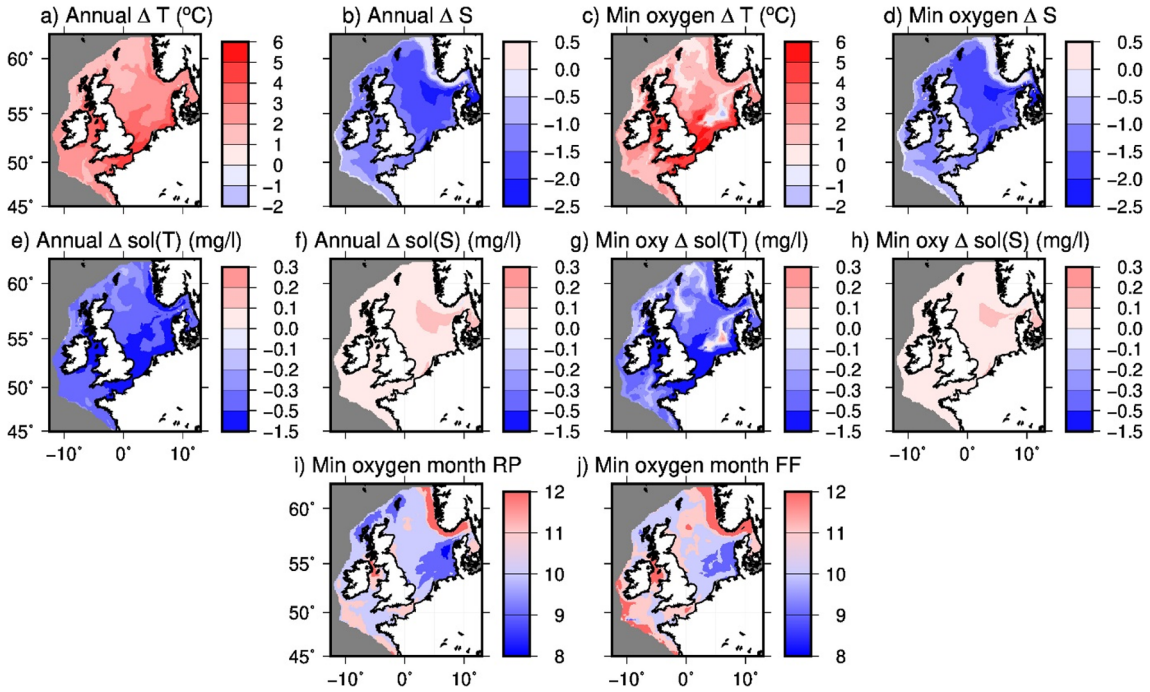

Fig. 12. The change in mean near bed a) temperature and b) salinity between the far future (FF, 2070–2099) and the recent past (RP, 1980–2009); the change in c) near bed temperature and d) near bed salinity between FF and RP in the calendar month for which near bed oxygen concentrations are minimum; e), f), g) and h) changes in oxygen solubility corresponding to a), b), c) and d), respectively, with salinity (e and g) or temperature (f and h) constant at RP values; and the month of year when the near bed oxygen minima occur in i) the RP and j) the FF.

North Sea, Skagerrak/Kattegat and Norwegian Trench have an impact as large as the solubility effect and also act to reduce oxygen concentrations due to increasing netPP fuelling increased near-bed bacterial respiration. These regions are strongly impacted by a reduction in the North Sea circulation at around 2040 which increases the nutrient concentrations from river sources. In more western regions of the NWES, the ecosystem mitigates the effect of the temperature/salinity changes and acts to increase oxygen concentrations; increasing oceanic stratification reduces nutrient supply here and leads to reduced primary production. Changes in the minimum monthly concentration is more strongly influenced by the ecosystem than is the annual mean oxygen.

In some regions of the NWES, the reduction in minimum near bed oxygen concentrations due to temperature and salinity climate changes was mitigated by ecosystem effects. The impact of climate change on oxygen concentrations could potentially be reduced by management policies affecting the ecosystem. For example, under the SRES A1B climate scenario, [Wakelin et al., 2015] found that reducing river nitrate and phosphate loads by 50% changed a projected increase in netPP by 2098 to a situation where there was either no significant change or a reduction in netPP in the southern half of the North Sea. In the eastern part of this area (region 3 in Fig. 1), the minimum near bed oxygen change is dominated by the ecosystem component (77% of the total change) so that cutting river nutrient loads thereby reducing netPP could potentially significantly impact the minimum oxygen concentration.

The method to separate temperature/salinity effects on near-bed oxygen from those due to the changing ecosystem gives an insight into the magnitudes and time evolutions of the different components of oxygen response to climate change. In the climate projection to 2100, the physical changes (temperature and salinity) affecting gas solubility are the dominant component of near bed oxygen reductions in many regions of the NWES. However, in the eastern North Sea changing ecosystem processes, acting to reduce oxygen concentrations, dominate. The Armorican Shelf and Celtic Sea also experience increasing oxygen depletion in the future but here the ecosystem processes partially mitigate the reductions due to solubility changes. Over the 21st century the mean oxygen concentration on the NWES is projected to decline by 6.3%, solubility changes forced by warming and freshening of the shelf water contribute 73% of the total change and the remainder is due to changes in the ecosystem. For monthly minimum oxygen the decline is 7.7% of which the solubility component is 50% of the total. These oxygen reductions might underestimate the impact of climate changes since oxygen concentrations increased in the CTL simulation testing for model drift.

In this study we used a single simulation of the northwest European shelf and surrounding ocean under a 'business as usual' future climate scenario. Where climate change impacts could not readily be estimated, e.g. in river flows and nutrient loads and atmospheric nitrogen deposition, we used values consistent with the present day so that potential impacts of climate variability from these sources are not included. Oxygen was not used as an open boundary condition so that changes in open ocean oxygen are not included. Potential adaptation of the ecosystem to changing climate is also not considered. The feasibility and likelihood of the results can only be determined by generating an ensemble of simulations under different climate scenarios and addressing other sources of model uncertainty, such as those due to model spin up, and model parameter setup. This is the subject of on-going work. However, this study produced a plausible and consistent climate projection for the northwest European shelf which was used to project changes in near bed oxygen concentrations and estimate the relative solubility/ecosystem contributions to that change.

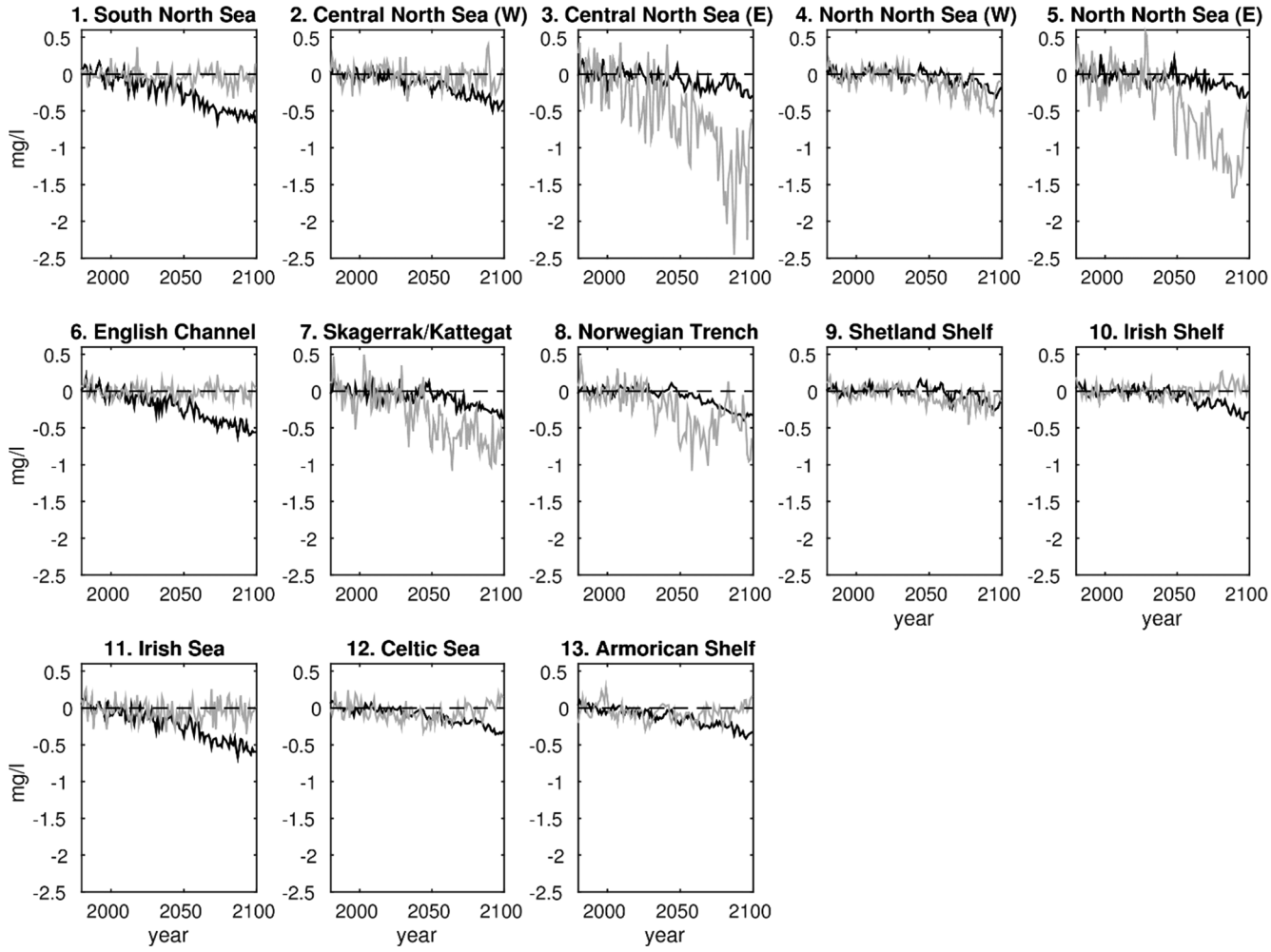

Fig. 13. Annual minimum near bed oxygen concentration change due to temperature/salinity changes ($\Delta DO_p^{\min}$, black line) and the change due to evolving ecosystem processes ($\Delta DO_e^{\min}$, grey line) for the 13 regions defined in Fig. 1.

Author contributions

SLW, YA and MB setup and performed the model simulations. SLW analysed data and drafted the manuscript. JTH and JB were project PIs. All authors contributed to the conception of the work, edited the manuscript and approved the final version.

Declaration of Competing Interest

The authors declare that they have no known competing financial interests or personal relationships that could have appeared to influence the work reported in this paper.

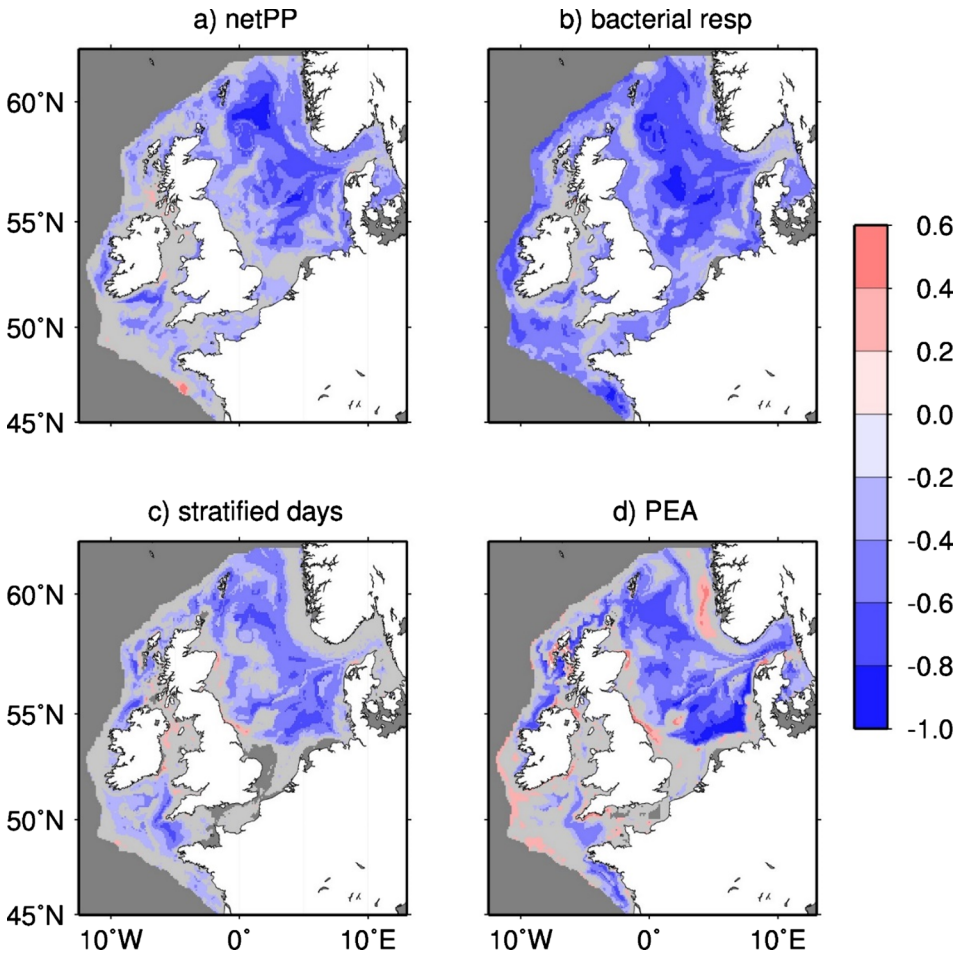

Fig. 14. Correlation between the ecosystem-related annual minimum oxygen ΔDO_e^{min} and a) water column integrated net primary production, b) near bed bacterial respiration, c) the annual number of stratified days and d) the potential energy anomaly (PEA). Net primary production and bacterial respiration are integrated from January to the month that the oxygen minimum occurs and PEA is averaged over the month of minimum oxygen concentration. Linear trends are removed from the time series at each point. The dark grey colour denotes off-shelf regions and shelf regions that do not seasonally stratify; areas where the correlation is not 99% significant are coloured light grey.

Acknowledgements

This work was supported by NOC and PML's National Capability program in Ocean Modelling and by funding from Natural Environment Research Council (NERC) research grants for ROAM (NE/H01733X/1, NE/H017372/1) and ReCICLE (NE/M003477/1). This work used the ARCHER UK National Supercomputing Service (http://www.archer.ac.uk). Monthly means of model data used in this paper are available at http://doi.org/10.5281/zenodo.3953801.

Appendix A. Model skill

A.1 Model validation

For climate models, a direct comparison with contemporary data is not possible because such models do not reproduce the actual phase of natural variability. Here we assess the mean conditions for the hindcast and the recent past (1980–2009) of the RCP8.5 climate simulation compared to climatologies generated using observations from the World Ocean Database (WOD) [Boyer et al., 2013]. Model climatologies for temperature, salinity and oxygen are calculated as annual cycles of mean monthly values on the model grid. Observations are gridded to the model grid and averaged over the model periods (1980–2009 for RCP8.5 and 1980–2007 for the hindcast) to give annual cycles of mean monthly values for comparison. Averaging over the model period maximises the number of data points that are available for comparison but may introduce biases in regions that are not frequently sampled (e.g. if for a particular month the observations in a grid cell do not span the whole month).

In all regions of the shelf (1–13, Fig. 1), both the hindcast and RCP8.5 temperature fields are warm compared to observations (Table A1); shelf-mean biases are 0.4 °C and 0.8 °C, respectively. Except for the Norwegian Trench and Skagerrak/Kattegat regions, the simulations are generally too fresh with shelf-mean biases of −0.1 (hindcast) and −0.2 (RCP8.5). Oxygen concentrations are mostly too low in both simulations, with shelf-mean biases of $-0.6\ mg\ l^{-1}$ (hindcast) and $-0.5\ mg\ l^{-1}$ (RCP8.5). Root-mean-square (RMS) differences for RCP8.5 are generally greater than those of the hindcast; the climate model is not constrained by observations and is unable to capture long period natural variability that might be present. RMS differences in the Skagerrak/Kattegat are higher than in the other regions due to the proximity of the model Baltic boundary; results in this region are therefore less certain than in the rest of the domain. Shelf-mean RMS differences for temperature are 1.2 °C (hindcast) and 1.5 °C (RCP8.5) and for salinity 0.8 (both simulations).

Table A1
Mean bias (model – observations), root-mean-square (RMS) differences and correlations between monthly mean model climatology and a climatology of gridded monthly mean observations for the hindcast and RCP8.5, averaged over regions of the European Shelf (Fig. 1).

	Temperature			Salinity			Oxygen		
	Bias (°C)	RMS (°C)	corr	bias	RMS	corr	bias (mg l^{-1})	RMS (mg l^{-1})	corr
hindcast (1980–2007)									
1. South North Sea	0.0	1.4	1.0	−0.6	1.4	0.8	−0.6	1.1	0.7
2. Central North Sea (W)	0.4	1.1	0.9	0.0	0.2	0.7	−0.6	0.9	0.6
3. Central North Sea (E)	0.3	1.5	0.9	−0.1	0.4	0.8	−0.5	1.1	0.6
4. North North Sea (W)	0.3	0.8	0.9	0.0	0.2	0.7	−0.5	0.9	0.6
5. North North Sea (E)	0.5	1.2	0.9	0.1	0.5	0.7	−0.6	0.8	0.7
6. English Channel	0.4	1.1	0.9	−0.3	1.4	0.7	−0.8	1.0	0.5
7. Skagerrak/Kattegat	0.6	1.7	0.9	0.5	2.4	0.9	−0.5	1.4	0.5
8. Norwegian Trench	0.7	1.3	0.9	0.0	0.6	0.8	−0.7	1.0	0.6
9. Shetland Shelf	0.5	0.9	0.9	0.0	0.2	0.7	−0.4	1.4	0.2
10. Irish Shelf	0.4	0.9	0.9	0.0	0.3	0.8	−0.9	1.2	0.2
11. Irish Sea	0.4	1.0	1.0	0.1	0.6	0.7	−0.9	1.2	0.1
12. Celtic Sea	0.5	1.1	0.9	−0.1	0.3	0.7	−0.6	0.8	0.5
13. Armorican Shelf	0.8	1.5	0.9	−0.4	0.7	0.7	−0.2	1.2	0.2
RCP8.5 (1980–2009)									
1. South North Sea	0.8	1.8	1.0	−1.0	1.6	0.8	−0.4	1.4	0.5
2. Central North Sea (W)	1.1	1.6	0.9	−0.1	0.2	0.7	−0.5	1.1	0.4
3. Central North Sea (E)	0.5	1.5	0.9	−0.4	0.6	0.8	−0.4	1.2	0.5
4. North North Sea (W)	0.8	1.2	0.9	−0.1	0.2	0.8	−0.4	1.0	0.5
5. North North Sea (E)	0.7	1.3	0.9	0.0	0.5	0.7	−0.5	1.0	0.6
6. English Channel	1.2	1.7	0.9	−0.5	1.5	0.7	−0.4	0.6	0.7
7. Skagerrak/Kattegat	1.3	2.2	0.9	0.3	2.1	0.9	−0.5	1.9	0.2
8. Norwegian Trench	0.9	1.4	0.9	0.0	0.6	0.9	−0.9	1.4	0.3
9. Shetland Shelf	0.7	1.0	0.9	−0.1	0.2	0.7	−0.4	1.4	0.2
10. Irish Shelf	0.7	1.2	0.9	−0.2	0.4	0.8	−1.2	1.7	0.0
11. Irish Sea	1.3	1.8	0.9	0.1	0.6	0.7	−1.5	1.9	−0.2
12. Celtic Sea	0.4	1.1	0.9	−0.2	0.4	0.7	−0.5	0.8	0.5
13. Armorican Shelf	0.9	1.6	0.9	−0.6	0.8	0.7	0.2	1.3	0.2

The correlation between model data and observations measures both the spatial agreement and the ability of the model to represent timing and change during a mean annual cycle. In all regions (Table A1) both simulations had very high (> 0.9) correlations for temperature and high (> 0.7) correlations for salinity. For oxygen, correlations were not significant for the Irish Sea and Irish shelf for RCP8.5, although all other regional correlations of 0.2–0.7 were significant.

A.2 Trends in temperature, salinity and oxygen

In the CTL simulation, regional averages (Fig. 3) of sea surface temperature (SST) and near bed temperature (NBT) are almost constant in time, with average linear trends of -2.1×10^{-4} to 4.7×10^{-4} °C decade^{-1} (SST) and -9.1×10^{-5} to 8.0×10^{-4} °C decade^{-1} (NBT). These trends are three orders of magnitude smaller than those of the RCP8.5 simulation, which are 0.24–0.45 °C decade^{-1} (SST) and 0.17–0.44 °C decade^{-1} (NBT). Using the Mann-Kendall non-parametric test for trend analysis [Kendall, 1975; Mann, 1945] the regional mean SST and NBT trends are significant for RCP8.5 but not for CTL at the 95% confidence level.

Regional averages of near bed salinity (NBS) and sea surface salinity (SSS) for CTL (Fig. 4) have no significant trends (with range -3.2×10^{-4} to 1.4×10^{-3} decade^{-1} for NBS and -2.4×10^{-4} to 1.4×10^{-3} decade^{-1} for SSS), whereas the RCP8.5 trends of −0.20 to −0.07 (NBS) and −0.30 to −0.10 decade^{-1} (SSS) are significant in each region with 95% confidence.

Regionally averaged near bed oxygen concentrations (Fig. 5) have trends with smaller magnitudes in CTL (3.3×10^{-5} to 1.6×10^{-2} mg l^{-1} decade^{-1}) than in RCP8.5 (-1.2×10^{-1} to -2.8×10^{-2} mg l^{-1} decade^{-1}). In all regions the CTL trend is positive while the RCP8.5 trend is negative, indicating that RCP8.5 might underestimate the impact of climate-forced changes. Using the Mann-Kendall non-parametric test for trend analysis, RCP8.5 trends are significant in all regions and, except for in the southern North Sea, the English Channel and the Irish Sea, the CTL trends are also significant. The significant CTL trends in some regions are probably due to aggregating errors in the ecosystem model, but could also be a consequence of a long-term slow process occurring in the benthos. The Celtic Sea (13% of the magnitude of RCP8.5) and Armorican Shelf (39% of RCP8.5), are additionally affected by close proximity to and transport from the open ocean, where the ecosystem model is still adjusting to the initial condition in the deeper water. The magnitudes of the CTL trends are less than 2% of those of RCP8.5 in eight of the regions and ~6 to 8% in the final three regions, and so are generally small compared to the RCP8.5 trends.

References

Baretta, J.W., Ebenhöh, W., Ruardij, P., 1995. The European regional seas ecosystem model, a complex marine ecosystem model. Neth. J. Sea Res. 33, 233–246.

Bindoff, N.L., Cheung, W.W., Kairo, J.G., Arístegui, J., et al., 2019. Chapter 5: Changing ocean, marine ecosystems, and dependent communities. In: H.-O. R. Pörtner, D.C., Masson-Delmotte, V., Zhai, P., et al. (Eds.), IPCC Special Report on the Ocean and Cryosphere in a Changing Climate (in press).

Blackford, J.C., Allen, J.I., Gilbert, F.J., 2004. Ecosystem dynamics at six contrasting sites: a generic modelling study. J. Mar. Syst. 52 (1–4), 191–215. https://doi.org/10.1016/j.jmarsys.2004.02.004.

Blaker, A.T., Hirschi, J.J.M., McCarthy, G., Sinha, B., Taws, S., Marsh, R., Coward, A., de Cuevas, B., 2015. Historical analogues of the recent extreme minima observed in the Atlantic meridional overturning circulation at 26°N. Clim. Dyn. 44 (1), 457–473. https://doi.org/10.1007/s00382-014-2274-6.

Boyer, T.P., Antonov, J.I., Baranova, O.K., Coleman, C., Garcia, H.E., Grodsky, A., Johnson, D.R., Locarnini, R.A., Mishonov, A.V., O'Brien, T.D., Paver, C.R., Reagan, J. R., Seidov, D., Smolyar, I.V., Zweng, M.M., 2013. World Ocean Database 2013, NOAA Atlas NESDIS, edited by E. S. Levitus, A. Mishonov, Technical Ed.; Silver Spring, p.

209.
Breitburg, D., Levin, L.A., Oschlies, A., Grégoire, M., Chavez, F.P., Conley, D.J., Garçon, V., Gilbert, D., Gutiérrez, D., Isensee, K., Jacinto, G.S., Limburg, K.E., Montes, I., Naqvi, S.W.A., Pitcher, G.C., Rabalais, N.N., Roman, M.R., Rose, K.A., Seibel, B.A., Telszewski, M., Yasuhara, M., Zhang, J., 2018. Declining oxygen in the global ocean and coastal waters. Science 359 (6371), eaam7240. https://doi.org/10.1126/science.aam7240.
Brown, J., Gmitrowicz, E.M., 1995. Observations of the transverse structure and dynamics of the low frequency flow through the North Channel of the Irish Sea. Cont. Shelf Res. 15 (9), 1133–1156. https://doi.org/10.1016/0278-4343(94)00063-S.
Brown, J., Carrillo, L., Fernand, L., Horsburgh, K.J., Hill, A.E., Young, E.F., Medler, K.J., 2003. Observations of the physical structure and seasonal jet-like circulation of the Celtic Sea and St. George's Channel of the Irish Sea. Continental Shelf Res. 23 (6), 533–561. https://doi.org/10.1016/S0278-4343(03)00008-6.
Butenschön, M., Clark, J., Aldridge, J.N., Allen, J.I., Artioli, Y., Blackford, J., Bruggeman, J., Cazenave, P., Ciavatta, S., Kay, S., Lessin, G., van Leeuwen, S., van der Molen, J., de Mora, L., Polimene, L., Sailley, S., Stephens, N., Torres, R., 2016. ERSEM 15.06: a generic model for marine biogeochemistry and the ecosystem dynamics of the lower trophic levels. Geosci. Model Dev. 9 (4), 1293–1339. https://doi.org/10.5194/gmd-9-1293-2016.
Capet, A., Beckers, J.M., Grégoire, M., 2013. Drivers, mechanisms and long-term variability of seasonal hypoxia on the Black Sea northwestern shelf – is there any recovery after eutrophication? Biogeosciences 10 (6), 3943–3962. https://doi.org/10.5194/bg-10-3943-2013.
Carstensen, J., Andersen, J.H., Gustafsson, B.G., Conley, D.J., 2014. Deoxygenation of the Baltic Sea during the last century. Proc. Natl. Acad. Sci. 111 (15), 5628–5633. https://doi.org/10.1073/pnas.1323156111.
Ciavatta, S., Kay, S., Saux-Picart, S., Butenschön, M., Allen, J.I., 2016. Decadal reanalysis of biogeochemical indicators and fluxes in the North West European shelf-sea ecosystem. J. Geophys. Res. Oceans 121 (3), 1824–1845. https://doi.org/10.1002/2015jc011496.
Cocco, V., Joos, F., Steinacher, M., Frölicher, T.L., Bopp, L., Dunne, J., Gehlen, M., Heinze, C., Orr, J., Oschlies, A., Schneider, B., Segschneider, J., Tjiputra, J., 2013. Oxygen and indicators of stress for marine life in multi-model global warming projections. Biogeosciences 10 (3), 1849–1868. https://doi.org/10.5194/bg-10-1849-2013.
Dee, D.P., Uppala, S.M., Simmons, A.J., Berrisford, P., Poli, P., Kobayashi, S., Andrae, U., Balmaseda, M.A., Balsamo, G., Bauer, P., Bechtold, P., Beljaars, A.C.M., van de Berg, L., Bidlot, J., Bormann, N., Delsol, C., Dragani, R., Fuentes, M., Geer, A.J., Haimberger, L., Healy, S.B., Hersbach, H., Hólm, E.V., Isaksen, L., Kållberg, P., Köhler, M., Matricardi, M., McNally, A.P., Monge-Sanz, B.M., Morcrette, J.J., Park, B.K., Peubey, C., de Rosnay, P., Tavolato, C., Thépaut, J.N., Vitart, F., 2011. The ERA-Interim reanalysis: configuration and performance of the data assimilation system. Q. J. R. Meteorolog. Soc. 137 (656), 553–597. https://doi.org/10.1002/qj.828.
Edwards, K.P., Barciela, R., Butenschön, M., 2012. Validation of the NEMO-ERSEM operational ecosystem model for the North West European Continental Shelf. Ocean Sci. 8 (6), 983–1000. https://doi.org/10.5194/os-8-983-2012.
Fairall, C.W., Bradley, E.F., Hare, J.E., Grachev, A.A., Edson, J.B., 2003. Bulk parameterization of air-sea fluxes: updates and verification for the COARE algorithm. J. Clim. 16 (4), 571–591. https://doi.org/10.1175/1520-0442(2003)016<0571:bpoasf>2.0.co;2.
Flather, R.A., 1981. Results from a model of the northeast Atlantic relating to the Norwegian Coastal Current. In: Saetre, R., Mork, M. (Eds.), The Norwegian Coastal Current. Bergen University, Bergen, Norway, pp. 427–458.
Garcia, H.E., Locarnini, R.A., Boyer, T.P., Antonov, J.I., 2006. World Ocean Atlas 2005, Volume 4: Nutrients (phosphate, nitrate, silicate). S. Levitus, Ed. NOAA Atlas NESDIS 64, U.S. Government Printing Office, Washington, D.C., 396 pp.
Gilbert, D., Rabalais, N.N., Díaz, R.J., Zhang, J., 2010. Evidence for greater oxygen decline rates in the coastal ocean than in the open ocean. Biogeosciences 7 (7), 2283–2296. https://doi.org/10.5194/bg-7-2283-2010.
Gröger, M., Maier-Reimer, E., Mikolajewicz, U., Moll, A., Sein, D., 2013. NW European shelf under climate warming: implications for open ocean – shelf exchange, primary production, and carbon absorption. Biogeosciences 10 (6), 3767–3792. https://doi.org/10.5194/bg-10-3767-2013.
Große, F., Greenwood, N., Kreus, M., Lenhart, H.J., Machoczek, D., Pätsch, J., Salt, L., Thomas, H., 2016. Looking beyond stratification: a model-based analysis of the biological drivers of oxygen deficiency in the North Sea. Biogeosciences 13 (8), 2511–2535. https://doi.org/10.5194/bg-13-2511-2016.
Helm, K.P., Bindoff, N.L., Church, J.A., 2011. Observed decreases in oxygen content of the global ocean. Geophys. Res. Lett. 38 (23). https://doi.org/10.1029/2011gl049513.
Holt, J., Wakelin, S., Lowe, J., Tinker, J., 2010. The potential impacts of climate change on the hydrography of the northwest European continental shelf. Prog. Oceanogr. 86 (3), 361–379. https://doi.org/10.1016/j.pocean.2010.05.003.
Holt, J., Butenschön, M., Wakelin, S.L., Artioli, Y., Allen, J.I., 2012. Oceanic controls on the primary production of the northwest European continental shelf: model experiments under recent past conditions and a potential future scenario. Biogeosciences J1 - BG 9 (1), 97–117. https://doi.org/10.5194/bg-9-97-2012.
Holt, J., Polton, J., Huthnance, J., Wakelin, S., O'Dea, E., Harle, J., Yool, A., Artioli, Y., Blackford, J., Siddorn, J., Inall, M., 2018. Climate-driven change in the North Atlantic and Arctic Oceans Can Greatly Reduce the Circulation of the North Sea. 11,827–811,836. Geophys. Res. Lett. 45 (21). https://doi.org/10.1029/2018gl078878.
Huthnance, J.M., Holt, J.T., Wakelin, S.L., 2009. Deep ocean exchange with west-European shelf seas. Ocean Sci. 5 (4), 621–634. https://doi.org/10.5194/os-5-621-2009.
IPCC, 2019. IPCC Special Report on the Ocean and Cryosphere in a Changing Climate. Edited by H.-O. R. Pörtner, D.C.; Masson-Delmotte, V.; Zhai, P.; et al. (in press).
Jones, C.D., Hughes, J.K., Bellouin, N., Hardiman, S.C., Jones, G.S., Knight, J., Liddicoat, S., O'Connor, F.M., Andres, R.J., Bell, C., Boo, K.O., Bozzo, A., Butchart, N., Cadule, P., Corbin, K.D., Doutriaux-Boucher, M., Friedlingstein, P., Gornall, J., Gray, L., Halloran, P.R., Hurtt, G., Ingram, W.J., Lamarque, J.F., Law, R.M., Meinshausen, M., Osprey, S., Palin, E.J., Parsons Chini, L., Raddatz, T., Sanderson, M.G., Sellar, A.A., Schurer, A., Valdes, P., Wood, N., Woodward, S., Yoshioka, M., Zerroukat, M., 2011. The HadGEM2-ES implementation of CMIP5 centennial simulations. Geosci. Model Dev. 4 (3), 543–570. https://doi.org/10.5194/gmd-4-543-2011.
Keeling, R.F., Körtzinger, A., Gruber, N., 2010. Ocean deoxygenation in a warming world. Ann. Rev. Mar. Sci. 2 (1), 199–229. https://doi.org/10.1146/annurev.marine.010908.163855.
Kendall, M., 1975. Rank Correlation Methods, 4th ed. London, Charles Griffith.
Key, R.M., Kozyr, A., Sabine, C.L., Lee, K., Wanninkhof, R., Bullister, J.L., Feely, R.A., Millero, F.J., Mordy, C., Peng, T.H., 2004. A global ocean carbon climatology: Results from Global Data Analysis Project (GLODAP). Global Biogeochemical Cycles 18 (4). https://doi.org/10.1029/2004gb002247. GB4031.
Knight, P.J., Howarth, M.J., 1999. The flow through the north channel of the Irish Sea. Cont. Shelf Res. 19 (5), 693–716. https://doi.org/10.1016/S0278-4343(98)00110-1.
Laurent, A., Fennel, K., Ko, D.S., Lehrter, J., 2018. Climate change projected to exacerbate impacts of coastal eutrophication in the Northern Gulf of Mexico. J. Geophys. Res. Oceans 123 (5), 3408–3426. https://doi.org/10.1002/2017jc013583.
Lavín, A., Valdés, L., Sánchez, F., Abaunza, P., Forest, A., Boucher, J., Lazure, P., Jegou, A. M., 2006. The Bay of Biscay: the encountering of the ocean and the shelf. In: Robinson, A., Brink, K. (Eds.), The Sea, Harvard University Press, pp. 933-999.
Lenhart, H.-J., Mills, D.K., Baretta-Bekker, H., van Leeuwen, S.M., der Molen, J.V., Baretta, J.W., Blaas, M., Desmit, X., Kühn, W., Lacroix, G., Los, H.J., Ménesguen, A., Neves, R., Proctor, R., Ruardij, P., Skogen, M.D., Vanhoutte-Brunier, A., Villars, M.T., Wakelin, S.L., 2010. Predicting the consequences of nutrient reduction on the eutrophication status of the North Sea. J. Mar. Syst. 81 (1–2), 148–170. https://doi.org/10.1016/j.jmarsys.2009.12.014.
Madec, G., 2008. NEMO ocean engine, Note du Pôle de modélisation, Institut Pierre-Simon Laplace (IPSL), France, No 27, ISSN No 1288-1619.
Mann, H.B., 1945. Nonparametric tests against trend. Econometrica 13 (3), 245–259. https://doi.org/10.2307/1907187.
O'Dea, E.J., Arnold, A.K., Edwards, K.P., Furner, R., Hyder, P., Martin, M.J., Siddorn, J.R., Storkey, D., While, J., Holt, J.T., Liu, H., 2012. An operational ocean forecast system incorporating NEMO and SST data assimilation for the tidally driven European North-West shelf. J. Oper. Oceanogr. 5 (1), 3–17.
OSPAR, 2000. Quality Status Report 2000, OSPAR Commission, London, 108 + vii pp, doi: https://qsr2010.ospar.org/media/assessments/QSR_2000.pdf.
OSPAR, 2003. Integrated Report 2003 on the Eutrophication Status of the OSPAR Maritime Area Based Upon the First Application of the Comprehensive Procedure, OSPAR Commission, Eutrophication Series, Publication nr. 189, ISBN 1-904426-25-5, download available at www.ospar.org.
Pätsch, J., Lenhart, H.J., 2004. Daily Loads of Nutrients, Total Alkalinity, Dissolved Inorganic Carbon and Dissolved Organic Carbon of the European continental rivers for the years 1977–2002, Berichte aus dem Zentrum fur. Meeres- und Klimaforschung; Reihe B: Oxeanographie 48, 159 pp.
Prandle, D., Ballard, G., Flatt, D., Harrison, A.J., Jones, S.E., Knight, P.J., Loch, S., McManus, J., Player, R., Tappin, A., 1996. Combining modelling and monitoring to determine fluxes of water, dissolved and particulate metals through the Dover Strait. Cont. Shelf Res. 16 (2), 237–257. https://doi.org/10.1016/0278-4343(95)00009-P.
Rabalais, N.N., Turner, R.E., Sen Gupta, B.K., Boesch, D.F., Chapman, P., Murrell, M.C., 2007. Hypoxia in the northern Gulf of Mexico: Does the science support the Plan to Reduce, Mitigate, and Control Hypoxia? Estuaries Coasts 30 (5), 753–772. https://doi.org/10.1007/bf02841332.
Riahi, K., Grübler, A., Nakicenovic, N., 2007. Scenarios of long-term socio-economic and environmental development under climate stabilization. Technol. Forecast. Soc. Chang. 74 (7), 887–935. https://doi.org/10.1016/j.techfore.2006.05.026.
Ruiz-Castillo, E., Sharples, J., Hopkins, J., Woodward, M., 2019. Seasonality in the cross-shelf physical structure of a temperate shelf sea and the implications for nitrate supply. Prog. Oceanogr. 177, 101985. https://doi.org/10.1016/j.pocean.2018.07.006.
Schmidtko, S., Stramma, L., Visbeck, M., 2017. Decline in global oceanic oxygen content during the past five decades. Nature 542, 335. https://doi.org/10.1038/nature21399.
Smyth, T.J., Moore, G.F., Hirata, T., Aiken, J., 2006. Semianalytical model for the derivation of ocean color inherent optical properties: description, implementation, and performance assessment. Appl. Opt. 45 (31), 8116–8131. https://doi.org/10.1364/AO.45.008116.
Song, Y., Haidvogel, D., 1994. A Semi-implicit Ocean Circulation Model Using a Generalized Topography-Following Coordinate System. J. Comput. Phys. 115 (1), 228–244. https://doi.org/10.1006/jcph.1994.1189.
Tinker, J., Lowe, J., Pardaens, A., Holt, J., Barciela, R., 2016. Uncertainty in climate projections for the 21st century northwest European shelf seas. Prog. Oceanogr. 148, 56–73. https://doi.org/10.1016/j.pocean.2016.09.003.
Topcu, H.D., Brockmann, U.H., 2015. Seasonal oxygen depletion in the North Sea, a review. Mar. Pollut. Bull. 99 (1), 5–27. https://doi.org/10.1016/j.marpolbul.2015.06.021.
Turrell, W.R., 1992. New hypotheses concerning the circulation of the northern North Sea and its relation to North Sea fish stock recruitment. ICES J. Mar. Sci. 49 (1), 107–123. https://doi.org/10.1093/icesjms/49.1.107.
van Vuuren, D.P., Edmonds, J., Kainuma, M., Riahi, K., Thomson, A., Hibbard, K., Hurtt, G.C., Kram, T., Krey, V., Lamarque, J.-F., Masui, T., Meinshausen, M., Nakicenovic, N., Smith, S.J., Rose, S.K., 2011. The representative concentration pathways: an

overview. Clim. Change 109 (1), 5. https://doi.org/10.1007/s10584-011-0148-z.
Vaquer-Sunyer, R., Duarte, C.M., 2008. Thresholds of hypoxia for marine biodiversity. PNAS 105 (40), 15452–15457. https://doi.org/10.1073/pnas.0803833105.
Vermaat, J.E., McQuatters-Gollop, A., Eleveld, M.A., Gilbert, A.J., 2008. Past, present and future nutrient loads of the North Sea: Causes and consequences. Estuar. Coast. Shelf Sci. 80 (1), 53–59. https://doi.org/10.1016/j.ecss.2008.07.005.
Vörösmarty, C.J., Fekete, B.M., Meybeck, M., Lammers, R.B., 2000. Global system of rivers: Its role in organizing continental land mass and defining land-to-ocean linkages. Global Biogeochem. Cycles 14 (2), 599–621. https://doi.org/10.1029/1999gb900092.
Wakelin, S.L., Artioli, Y., Butenschön, M., Allen, J.I., Holt, J.T., 2015. Modelling the combined impacts of climate change and direct anthropogenic drivers on the ecosystem of the northwest European continental shelf. J. Mar. Syst. 152, 51–63. https://doi.org/10.1016/j.jmarsys.2015.07.006.
Wakelin, S.L., Holt, J.T., Blackford, J.C., Allen, J.I., Butenschön, M., Artioli, Y., 2012. Modeling the carbon fluxes of the northwest European continental shelf: Validation and budgets. J. Geophys. Res. Oceans 117 (C5), C05020. https://doi.org/10.1029/2011JC007402.
Wanninkhof, R., 1992. Relationship between wind speed and gas exchange over the ocean. J. Geophys. Res. Oceans 97 (C5), 7373–7382. https://doi.org/10.1029/92jc00188.
Wanninkhof, R., McGillis, W.R., 1999. A cubic relationship between air-sea CO2 exchange and wind speed. Geophys. Res. Lett. 26 (13), 1889–1892. https://doi.org/10.1029/1999gl900363.
Weiss, R.F., 1970. The solubility of nitrogen, oxygen and argon in water and seawater. Deep Sea Res. Oceanogr. Abstracts 17 (4), 721–735. https://doi.org/10.1016/0011-7471(70)90037-9.
Yool, A., Popova, E.E., Coward, A.C., Bernie, D., Anderson, T.R., 2013. Climate change and ocean acidification impacts on lower trophic levels and the export of organic carbon to the deep ocean. Biogeosciences 10 (9), 5831–5854. https://doi.org/10.5194/bg-10-5831-2013.
Young, E.F., Holt, J.T., 2007. Prediction and analysis of long-term variability of temperature and salinity in the Irish Sea. J. Geophys. Res. Oceans 112 (C1), C01008. https://doi.org/10.1029/2005JC003386.